Response of hydrogeological processes in a regional groundwater system to environmental changes

A modeling study of Yinchuan Basin, China

Li, Jie; Zhou, Yangxiao; Wang, Wenke; Liu, Sida; Li, Ying; Wu, Ping

DOI
10.1016/j.jhydrol.2022.128619

Publication date
2022

Document Version
Final published version

Published in
Journal of Hydrology

Citation (APA)
Li, J., Zhou, Y., Wang, W., Liu, S., Li, Y., & Wu, P. (2022). Response of hydrogeological processes in a regional groundwater system to environmental changes: A modeling study of Yinchuan Basin, China. *Journal of Hydrology*, *615*, Article 128619. https://doi.org/10.1016/j.jhydrol.2022.128619

Journal of Hydrology 615 (2022) 128619

Contents lists available at ScienceDirect

Journal of Hydrology

journal homepage: www.elsevier.com/locate/jhydrol

Research papers

Response of hydrogeological processes in a regional groundwater system to environmental changes: A modeling study of Yinchuan Basin, China

Jie Li [a,b], Yangxiao Zhou [c,d], Wenke Wang [a,b,*], Sida Liu [c,e], Ying Li [f], Ping Wu [g]

[a] School of Water and Environment, Chang'an University, Xi'an 710054, China
[b] Key Laboratory of Subsurface Hydrology and Ecological Effects in Arid Region, Chang'an University, Xi'an 710054, China
[c] IHE Delft Institute for Water Education, 2611 AX Delft, The Netherlands
[d] School of Water Resources and Environment, Hebei GEO University, Shijiazhuang 050030, China
[e] Delft University of Technology, 2628 CN Delft, The Netherlands
[f] Geological Bureau of Ningxia Hui Autonomous Region, Yinchuan 750021, China
[g] Institute of Hydrogeology and Environmental Geology of Ningxia, Yinchuan 750011, China

ARTICLE INFO

Keywords:
Quaternary sediments, Yinchuan Basin
Numerical groundwater flow model
Human activities
Climate change
Surface water-groundwater interactions

ABSTRACT

The sustainable development of groundwater resources in arid and semi-arid regions is a challenging task hindered by climate change and human activities. The rational utilization and management of groundwater resources is, therefore, dependent on an understanding of the influences of human and climatic factors on the spatial distribution of groundwater resources and their change over time. The thick Quaternary aquifers in the Yinchuan Basin, China were used herein as an example of how to quantitatively assess spatial and temporal trends in groundwater resources in response to human activities and climate change. A 3D transient groundwater flow model was constructed and used to simulate the evolution and spatial variability of hydrogeological processes from 1990 to 2020. By subsequently applying regime shift detection and correlation analysis to the simulation results, we found that: 1) groundwater storage was continuously depleted over the 30-year period, reaching a cumulative depletion of 1.89×10^9 m^3; 2) human activities were mainly responsible for variations in regional hydrogeological processes for a period of up to 30 years. Climate only affected short-term interannual fluctuations in groundwater storage; 3) human activities (e.g., river water diversion and groundwater abstractions) were the decisive factors causing a continuous reduction of groundwater resources. A policy-driven reduction in water diversion from the Yellow River directly led to a significant drop in groundwater storage, which had a consequent effect on surface water and groundwater interactions and altered agricultural irrigation patterns (crop patterns and irrigation methods); 4) the amount of groundwater recharge from the Yellow River and local lakes increased from 1990 to 2020, whereas the discharge of groundwater to the Yellow River and lakes decreased.

1. Introduction

Groundwater is a crucial component of regional water cycles and plays a vital role in regional socio-economic development and ecosystem conservation, especially in arid and semi-arid regions characterized by scarce precipitation and surface water resources, strong evapotranspiration, and fragile ecosystems. Groundwater is not only an important source of domestic, industrial, and agricultural water, but is also critical for maintaining ecosystems in arid areas (Wang et al., 2021a). For example, the growth of natural vegetation often depends on phreatic evapotranspiration, and the maintenance of the water levels, volumes and areas of rivers and lakes depends on the balance between groundwater recharge and discharge (Li et al., 2020a; Ma et al., 2022; Zhou et al., 2020). In recent decades, the impact of global climate change and human activities associated with rapid socio-economic development on hydrogeological processes has become increasingly prominent. Changes in climatic factors (e.g., precipitation and evapotranspiration) and human activities (e.g., agricultural irrigation and groundwater abstractions) have the potential to substantially affect hydrogeological processes and mechanisms (Fu et al., 2019; Liu et al., 2022; Meixner et al., 2016; Nofal et al., 2019; Ramos et al., 2020; Shamir et al., 2015; Taylor et al., 2013; Vrzel et al., 2019; Xu and Su, 2019).

* Corresponding author at: School of Water and Environment, Chang'an University, Xi'an 710054, Shaanxi, China.
E-mail address: wenkew@chd.edu.cn (W. Wang).

https://doi.org/10.1016/j.jhydrol.2022.128619
Received 11 August 2022; Received in revised form 20 September 2022; Accepted 21 September 2022
Available online 30 October 2022

Climate factors, including precipitation and evaporation, affect groundwater systems by altering the interactions between groundwater and surface water bodies (e.g., lakes and rivers) as well as by affecting recharge processes (Carlson et al., 2011; Jyrkama and Sykes, 2007). Human activities, in contrast, directly impact groundwater through the exploitation of groundwater resources and/or their influence on groundwater recharge. In addition, human activities may indirectly affect groundwater recharge/discharge as land use/cover is altered during the implementation of agricultural development projects, and/or by urbanization, among other activities (Zhang et al., 2014). Such human induced disturbances may lead to a sharp drop in groundwater levels, a change in the water cycle, and/or a deterioration of groundwater quality (Sekhar et al., 2013).

In semi-arid farmlands, irrigation return flow and canal leakage may greatly contribute to groundwater recharge (Jimenez-Martinez et al., 2010), especially when a large amount of water from a perennial river supplies the irrigation systems (Vallet-Coulomb et al., 2017). Therefore, groundwater flow and storage can change in response to alterations in agricultural irrigation, land use, and water demand. In this context, maintaining the long-term balance of groundwater systems is critical to supporting a sustainable economic and ecological environment (Fu et al., 2019). Given the complexity of the system, and the wide range of factors that may impact groundwater systems, the sustainable management of groundwater resources is an arduous issue that requires an evaluation of hydrogeological processes, an analysis of natural and anthropogenic drivers, and an understanding of the mechanisms controlling the regional water cycle.

Understanding the impacts of environmental change on groundwater systems requires, on the one hand, an assessment of the evolution of the numerous interacting hydrogeological variables that control the groundwater system (e.g., river stages, lake water levels, and lateral boundary flow). On the other hand, it is necessary to evaluate alterations in climate and human activities that represent the primary controls on groundwater (e.g., precipitation, evapotranspiration, crop patterns, the intensity of extraction and water allocation policy). However, the proper evaluation of different types of variables is often complex and indistinguishable as they are related to multiple physical factors with high temporal and spatial variability (Pulido-Velazquez et al., 2015). To address such research needs, a wide range of approaches have been applied, including water balance methods (Li et al., 2020a), statistical analyses (Hou et al., 2022; Wang et al., 2018), integrated hydrological modelling (MIKESHE, GSFLOW) (Feng et al., 2018), and numerical groundwater models (Liu et al., 2021; Ramos et al., 2020; Wang et al., 2021b; Zhou et al., 2020). Integrated hydrological modelling is often difficult to apply to large areas because of its extensive requirements for surface information and surface water parameters; it is also difficult to achieve a high level of accuracy with such hydrologic models. Numerical groundwater simulations are commonly used to evaluate the response of groundwater flow processes to climate change and anthropogenic disturbances. A transient groundwater flow model that describes the heterogeneous structure of the aquifer can provide important insights for the accurate evaluation, regulation, and management of groundwater resources. However, it is a challenge to characterize the heterogeneity of complex multi-layer hydrogeological structures in finite-difference grids with reasonable partitioning and stratification (Burns et al., 2010). The Hydrogeologic Unit Flow package (HUF) (Anderman and Hill, 2000) of MODFLOW-2005 (Harbaugh, 2005; Hill et al., 2000) can address this challenge. HUF allows hydrogeological units to be defined independently of model layers, eliminating the need to determine how to delineate model layers to match highly heterogeneous structures.

The Yinchuan Basin is an important food production area located in the arid and semi-arid region of northwest China. Due to the lack of local surface water resources and precipitation, socio-economic water demand mainly depends on the diversion of water from the Yellow River. More frequent droughts accompanied by a reduction in river flows have resulted in a lower water supply. As a result, groundwater abstractions from local and regional aquifers now serve as a secondary and stable source of water in the Yinchuan Basin. Moreover, during the past 30 years, the Yinchuan Basin has experienced accelerated urbanization and sustained population growth (NSB, 1991-2020). In 1990, 9.4 million people lived in the Yinchuan Basin. The population had grown to 11.1 million, 15.7 million and 17.5 million by 2000, 2010 and 2019, respectively (NSB, 1991-2020). As a result, the demand for groundwater for domestic, industrial, and agricultural purposes have (and continue) to increase. Moreover, changes in the mechanisms of water diversion, irrigation, and land use may have substantially modified hydrogeological processes. Therefore, the groundwater system of the Yinchuan Basin appears to be very sensitive to human activities.

Recent reductions in Yellow River discharges as a result of climate change and intensive human activities have also raised concerns about water availability in the Yinchuan Basin. Of particular concern is the amount of water that can be allocated from the Yellow River and the exploitable amount of groundwater in the coming years. To ensure the sustainable utilization of water resources in the Yinchuan Basin, it is necessary to investigate the simultaneous response of hydrogeological processes to long-term human activities and climate factors and to assess trends in the changes in groundwater recharge processes over time and space (Nofal et al., 2019). Previous water balance calculations and numerical groundwater simulations in the Yinchuan Basin have mainly focused on one or several temporal hydrological years, in which the exploitable amount and pollution potential of groundwater were the main concern (Li et al., 2020b; Qian et al., 2012; Xu et al., 2015). The groundwater response to long-term changes in climate and human activities and the complex interactions between the groundwater and surface systems have not been systematically studied.

This study adopts a transient groundwater flow simulation, based on the MODFLOW model, to assess the long-term hydrogeological processes, and the factors controlling these processes, within the thick unconsolidated Quaternary aquifers of the Yinchuan Basin from 1990 to 2020. The main objectives of the study are to: 1) detect the temporal and spatial trends in hydrogeological processes; 2) identify the trends and abrupt change points in climate change, human activities, and hydrogeological processes; 3) evaluate groundwater dynamics under the influence of natural forces (climate) and human-related forces (human activities); and 4) explore the response of groundwater-surface water interactions to long-term human activities and climate factors. The results of this study provide science-based information for the rational development of groundwater resources, help to design effective measures to cope with the impact of climate change and human activities, and formulate appropriate sustainable groundwater management plans in arid and semi-arid basins.

2. Materials and methods

2.1. Study area

The Yinchuan Basin is located in the northern Ningxia Hui Autonomous Region of China (Fig. 1). It is bounded by Qingtongxia Canyon to the south, the Ordos Platform to the east, and the Helan Mountains to the north and west. The basin varies in width from 10 to 60 km, and possesses a long axis, oriented nearly in a south-north direction, that is 181 km in length. The basin covers an area of approximately 7088 km^2, and has an elevation that ranges between 1100 m and 1300 m above sea level. Topography dips gently from southwest to northeast. Structurally, the Yinchuan Basin is a fault-controlled basin developed during the Cenozoic Era. High subsidence rates within the basin have allowed for the enhanced deposition of unconsolidated Quaternary sediments (Han et al., 2013), which reach about 1700 m in thickness within the center of the basin. These sediments become thinner towards the basin's margins (Yang et al., 2018).

Geomorphologically, the Yinchuan Basin can be subdivided into three topographic units, each of which is associated with a distinct

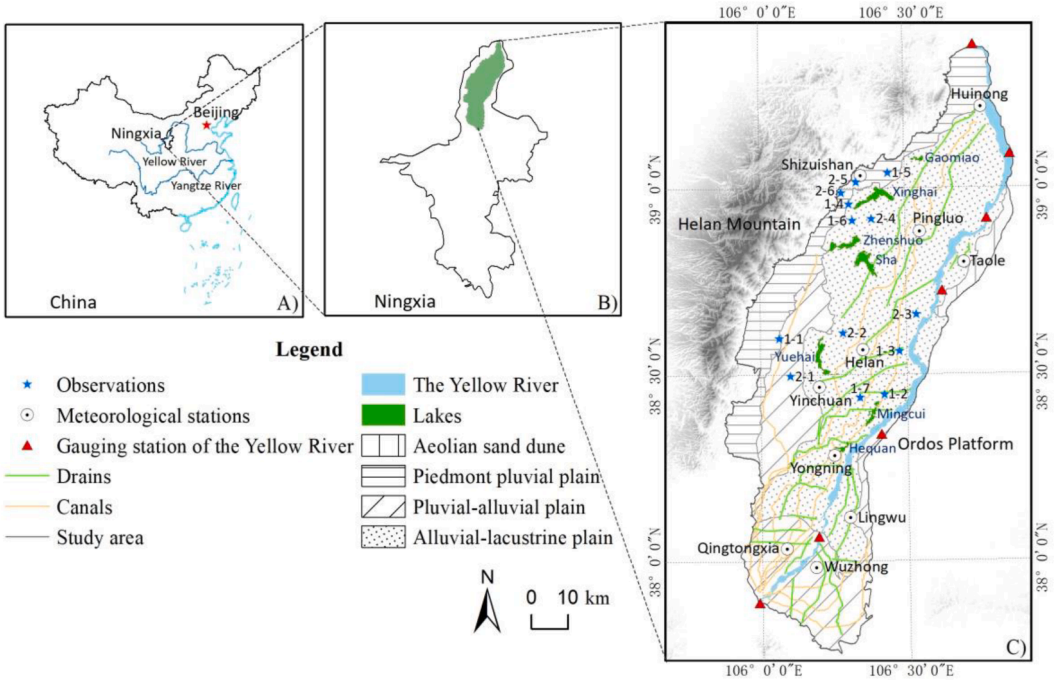

Fig. 1. Location of the Yinchuan Basin in A) China; B) the Ningxia Hui Autonomous Region; and C) the Yinchuan Basin.

sedimentary sequence: 1) A piedmont pluvial plain underlain predominantly by coarse (gravel-sized) sediments; 2) A pluvial-alluvial plain underlain by sandy gravel-sized sediments; and 3) An alluvial-lacustrine plain underlain by relative fine sediments, consisting primarily of sand, silt, and clay. Fine-grained sediments dominated by sandy clays are generally found along the piedmont pluvial front.

The Yinchuan Basin is characterized by arid and semi-arid conditions that are associated with a continental climate with sufficient sunshine, little rainfall, and strong evapotranspiration. Climatic data within the Yinchuan Basin have been collected from 1990 to 2019 at the Yinchuan station (Fig. 2). The mean annual precipitation is about 186 mm/a, with most rains occurring from May to September. The mean annual evapotranspiration is about 1748 mm (measured with a 20 cm evaporating dish, E601). Most evapotranspiration occurs between April and September. The annual evapotranspiration is about 10 times the annual precipitation. The monthly mean temperatures range from −7 to 24°C. The Yellow River is an important perennial river that flows through the Yinchuan Basin from southwest to northeast. It is the most important source of irrigation water; irrigation return flow serves as a major source of groundwater recharge (Mi et al., 2020).

Due to the unique geological structure, climate, and hydrogeological characteristics of the Yinchuan Basin, an "underground reservoir" of pore water exists within the thick unconsolidated Quaternary sediments in the basin. Groundwater is mainly recharged by irrigation return flow, canal leakage, precipitation infiltration, and lateral groundwater runoff from the foothills of the Helan Mountains. Groundwater is also recharged directly from the Yellow River, where the river stage is above the groundwater level. Groundwater is discharged into surface water bodies (including the drains, the Yellow River and lakes), or is lost via other outflow components including evapotranspiration and abstractions. Among these flow routes, irrigation return flow and drainage are the most important components effecting recharge and discharge of the groundwater system. The dominant groundwater flow direction in the study area is generally from the southwest to the northeast and is characterized by hydraulic gradients that exceed 0.04%. Beneath the northern alluvial-lacustrine plain, groundwater flows to the northeast under a hydraulic gradient lower than 0.04% due to the area's flat-lying topography before flowing into the Yellow River (Han et al., 2013). Except within the piedmont pluvial plain, the groundwater table in most parts of the basin is less than 3 m below the ground surface (Qian et al., 2014). Most of the lakes in the study area are distributed along linear depressions that represent the old route of the Yellow River. These lakes possess an obvious oxbow morphology. Other lakes are distributed in depressions in front of or between alluvial fans and are irregularly shaped (Zhang, 2007).

Most of the land in the Yinchuan Basin is cultivated for irrigated crops consisting mainly of rice, wheat, and corn. To compensate for the lack of rainfall, the crops are irrigated during the growing season with waters diverted mostly from the Yellow River. Additional irrigation water is obtained from groundwater withdrawals. Water from the Yellow River is transported from south to north to farmland through a canal system. Irrigation return water from the farmland is ultimately discharged back into the Yellow River through a network of drains.

Numerous water conservancy projects have been implemented in the area, most of which were constructed in the 1960s and 1970s. The constructed projects were restricted by economic conditions at the time; thus, the loss of diversion water by leakage is large. The region's convenient water diversion conditions favoured the use of traditional flood irrigation in the study area, an approach that is characterized by large water diversions and drainage. Large-scale water diversions for irrigation have also resulted in increased groundwater recharge and groundwater resources that have maintained local lakes and wetlands. Therefore, surface water and groundwater are closely related, leading local residents to say that "the water of the Yellow River enriches Ningxia", which comes in the form of local economic development. However, as a result of the diversions, runoff in the Yellow River declines significantly after it flows through the Yinchuan Basin.

2.2. *Construction of a conceptual hydrogeological model*

Development of the conceptual model consisted of three steps: 1) Construction of a 3D lithological model, 2) Creation of conceptual model coverages, and 3) Mapping of the conceptual model to MODFLOW numerical model packages.

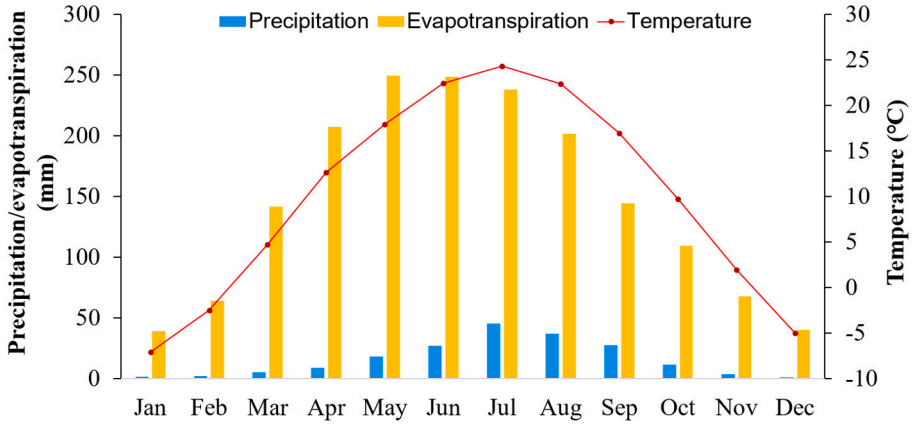

Fig. 2. Average monthly temperature, precipitation, and evapotranspiration over the 30-year study period (1990–2019).

2.2.1. A three-dimensional lithological model

A 3D lithological model of the study area was built using an integrated approach that had previously been used to construct a hydrogeological structure model of the basin's thick unconsolidated sediments (Li et al., 2021). The 3D lithological model is based on multiple sources of data (including borehole surface elevation data, borehole lithology data, audio-frequency magnetotelluric data (AMT), and lower boundary elevation data) for the Quaternary sediments that were integrated using several methods including Sequential Gaussian Simulation and Natural Neighbor Interpolation. The integrated geological model reproduces the spatial heterogeneity of the basin's geometric features and repeated geometric patterns.

2.2.2. Conceptual model coverages

The Groundwater Modeling System 10.4 (GMS10.4) was used to create conceptual model coverages, including:

1) Boundary coverages (arcs and properties).

The boundaries of the first layer in the Yinchuan Basin were defined as general head boundaries. The western boundary adjacent to the Helan Mountains was set as a highly permeable boundary that receives a supply of bedrock fissure water and terrestrial flood flows from the mountains. The boundaries to southwest and south were defined as weakly permeable boundaries associated with alluvial fans and a delta, respectively. The boundaries for layers 2–11 were generalized as no-flow boundaries. A no-flow boundary was also adopted for the bottom of the Quaternary sediments (Fig. 3).

2) Sources/sinks coverages.

A. Recharge from precipitation (Areal recharge coverage).

Monthly precipitation data between 1990 and 2020 from 10 meteorological stations (Fig. 1) were obtained from the Ningxia Meteorological Bureau. Thiessen polygons were used to calculate the control area of the 10 meteorological stations. The corresponding infiltration coefficients (Table 1) were then assigned to different soil types and land-use types on the basis of the soil zonation map of the vadose zone (obtained from the Institute of Hydrogeology and Environmental Geology of Ningxia). The recharge rate from precipitation was then calculated based on different zones using the following equation:

$$P_r = I^*P \tag{1}$$

where P_r (m/d) is the recharge rate from precipitation, P (m/d) is the monthly precipitation rate, and I (dimensionless) is the infiltration coefficient of the different soil types.

B. Irrigation return flow (Areal recharge coverage).

The zonation of irrigation return flow was based on an interpretation of administrative divisions, soil types, and land-use types as determined from a U.S. Landsat 30 m resolution image of the Yinchuan Basin acquired in 2018 (Xu et al., 2018). The recharge rate for irrigation return flow was calculated as:

$$I_r = U^*I^*W/A \tag{2}$$

where I_r (m/d) is the recharge rate of irrigation return flow, U (dimensionless) is the effective utilization coefficient of field water, I (dimensionless) is the infiltration coefficient of the different soil types, W (m^3/d) is the monthly agricultural water utilization from both the Yellow River and groundwater, and A (m^2) *is* the area of each zone. The agricultural water intake for each administrative division was obtained from the Ningxia Water Resources Bulletin (NWRD 2000-2020).

C. Canal leakage (Specified flow coverage).

The leakage rates of the canals (Fig. 3) were calculated by:

$$C_l = D_i^*(1 - C_u)^*C_i \tag{3}$$

where C_l (m^3/d) is the recharge rate from canal leakage, D_i (m^3/d) is the monthly water diversion from the Yellow River, C_u (dimensionless) is the effective utilization coefficient of canal water, and C_i (dimensionless) is the infiltration coefficient for the canals. Water diversions of each canal were obtained from the Ningxia Water Resources Bulletin (NWRD 2000-2020).

D. Groundwater abstractions (Well coverage).

Two types of groundwater abstractions were included in the coverages. The first is the centralized abstractions from the deep aquifer (layers 2–3), which was mainly used for industrial and urban water supplies. The second includes abstractions from the shallow aquifer (layer 1–2); these abstractions were primarily conducted through scattered wells (including hand- and motor-operated wells). The water from these wells is mainly used for agriculture and as a rural water supply. Where the pumping rate of a well field was not available, the pumping rate was defined as the allowable pumping rate of the well field. The allowable pumping rate specifies the maximum daily pumping rate for each well field. The pumping rates of scattered wells were assigned to the model according to the administrative division. The pumping rate of each administrative division was obtained from the Ningxia Water Resources Bulletin (NWRD 2000-2020).

E. Evapotranspiration (ET coverage).

The evapotranspiration rate of groundwater was estimated on the basis of calculated surface evapotranspiration as determined from a MOD16 data set. Zonation was then conducted on these estimates of evapotranspiration rate. The extinction depth of phreatic evapotranspiration was set as 3.1 m. The elevation of the ET surface was set as the land surface elevation.

F. Discharge from drainages (Drain coverage).

Excess irrigation water was drained and discharged to the Yellow River (Fig. 3). Drains were assigned a bottom elevation of 3 m below the surface. The conductivities of all drains were set to 12 m/d.

G. The Yellow River (General head coverage).

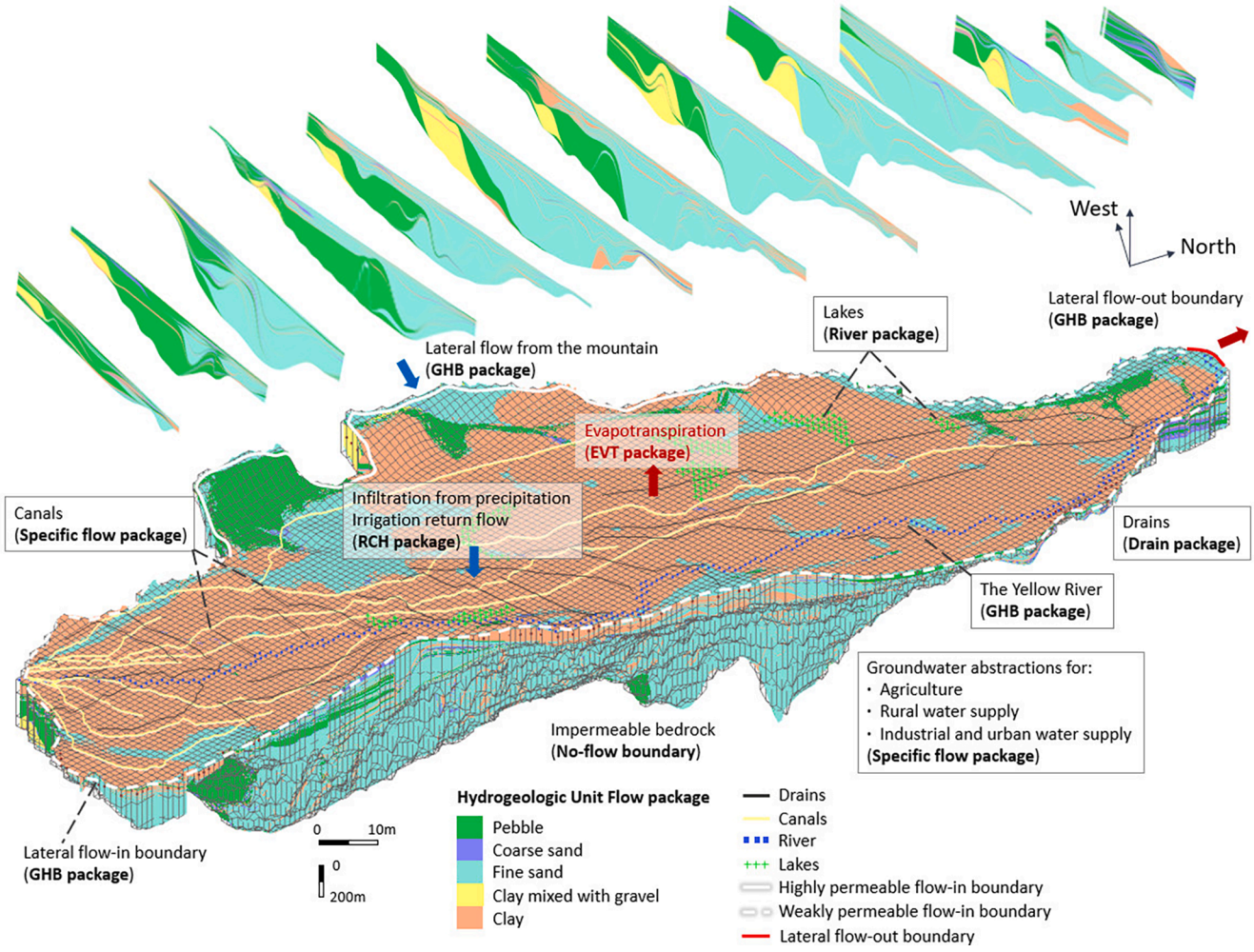

Fig. 3. Conceptual three-dimensional hydrogeological model showing hydrogeological units, boundary conditions, groundwater sources and sinks, and discretization across the study area.

Table 1
Infiltration coefficients for each soil and land-use type.

Soil type and land use	Infiltration coefficient
Clay	0.08
Sand	0.18
Pebble	0.30
Cities	0.00
Lakes and river	0.00

*The infiltration coefficients were obtained from the Handbook of Hydrogeology (CGS, 2012).

The monthly stages of the Yellow River as recorded at the Qingtongxia and Shizuishan Stations were obtained for the period of 1990 to 2020. The monthly Yellow River stages in 2000 were also collected from 5 additional gauging stations (Yesheng, Wuduizi, Shiba, Hongyazi and Gaorenzhen). The conductance of the riverbed material was set to 0.06 $m^2/d/m$.

H. Lakes (River coverage).

The location and geometry of 7 lakes with an area greater than 2.96 km^2 (Fig. 1) in the study area were extracted from remotely sensed images (Xu et al., 2018). The conductance of the lakebed material was set to 0.01 $m^2/d/m^2$. To maintain the stability of the ecological environment, the government replenishes the lakes through water diversions from the Yellow River. Therefore, the lake areas, water depths, and water surface elevation of the 7 lakes are relatively stable and were set as fixed values in our model. The head-stages and bottom elevations were based on survey data of average lake depth collected by the Institute of Hydrogeology and Environmental Geology of Ningxia. The general characteristics of the 7 lakes are shown in Table S1 in Supplementary.

3) Hydrogeological unit properties.

The initial hydraulic conductivities (horizontal and vertical) were assigned to each hydrogeological unit according to the results of pumping tests (GSIN, 2016). The initial specific storages and initial specific yields of each material were based on the Handbook of Hydrogeology (CGS, 2012). Those parameters were then calibrated in the model (Table 2).

4) Observation coverage.

Data from 201 long-term observation wells near Yinchuan City and Shizuishan City from 1990 to 2019 were obtained from the Ningxia Water Resources Department. Groundwater levels were measured monthly in most of these wells. In addition, surveillance measurements of groundwater levels were obtained for a large number of production and observation wells. In total, data were available for 1180 wells distributed in layers 1–3.

2.3. Construction of the numerical model

The transient groundwater flow model was established using Modflow-2005 (Harbaugh et al., 2017; Harbaugh, 2005). In 1990, the observed groundwater levels were relatively stable and precipitation was abundant. Therefore, a steady-state simulation for the year 1990

was first performed to conduct a preliminary calibration of hydrogeological parameters and determine the initial heads for the transient simulation covering the period from 1990 to 2020.

2.3.1. Model grid and stress period

A total of 372 monthly stress periods were defined for the simulated interval of January 1990 to December 2020. The y (north–south) and x (west-east) directions were evenly discretized with a fixed grid size of 1000 m by 1000 m. This created a model grid of 181 rows and 87 columns. Eleven layers were chosen for the model in the z (vertical) direction. The surface elevation and bottom elevation of the model were determined by the 3D geological structure model developed by Li (2021). The areal extension of the model layers was truncated by the bottom elevation of the basin (Aquaveo, 2017). Since the bottom of the model is "bowl-shaped", the number of grids within each model layer decreases sequentially from the top to the bottom. The first layer contains 7185 grid cells; the second layer contains 6891 grid cells. The 11 layers in total, contain 34,236 active grid cells. The first layer was set as unconfined, whereas the remaining layers were set as confined.

2.3.2. Model packages

1) Flow package: Hydrogeological unit flow package (HUF).

The study area is characterized by fluvial-lacustrine sedimentary facies (including river channel and flood deposits) that exhibit complex and highly heterogeneous geometries which appear in repeated patterns (Friend, 1983; Gibling, 2006; Miall, 2006). The Hydrogeological Unit Flow (HUF) package was used in MODFLOW-2005 (Anderman and Hill, 2000) to represent detailed stratigraphic profiles in the finite-difference grids. HUF can represent hydrogeological units with variable thickness and distribution, while supporting the attribute modeling of numerical layers of uniform thickness (Langevin et al., 2008). In general, HUF can more effectively describe vertical changes in the hydrogeological properties of the sediments than more traditional approaches.

By using HUF to establish the geometric structure of the hydrogeological units independently of the model layers, the hydraulic properties (Table 2) are directly assigned to hydrogeological units that are geometrically distinct from the model layers, rather than to grid cells. HUF calculates the effective hydraulic properties of each grid according to the top elevation and thickness of the hydrogeological units contained in the grids (Anderman and Hill, 2000).

2) Sources and sinks package.

The source and sink data used in the conceptual model coverages were mapped to MODFLOW packages of the numerical model (Table S2, Supplementary). Recharge from both precipitation and irrigation were assigned with the Recharge package. Canal leakage and abstractions were assigned using the Well package. ET was set by the Evapotranspiration package. Drains were defined in the Drain package. The Yellow River is in hydraulic contact with the aquifer and was simulated using the General Head Boundary (GHB) package. Lakes were simulated using the River package. Boundaries were set using the GHB package.

2.3.3. Model calibration

The hydrogeological parameters were calibrated manually based on data from the 201 long-sequence observation wells and the 979 wells where surveillance measurements of groundwater levels were obtained for different years and months. Calibration was conducted by adjusting several hydrogeological parameters within hydrogeologically reasonable limits until the simulated groundwater levels matched the observed groundwater levels. The mean absolute error (MAE), root mean squared error (RMSE), and coefficient of determination (R^2) were selected as indicators of goodness of fit.

2.4. Statistical analysis methods

Detection of shifts in means is the most common method used to identify abrupt change points. A Regime Shift Detection analysis (Rodionov and Overland, 2005), based on a sequential *t*-test analysis of regime shifts (STARS), was used to statistically detect the regime changes in major sources and sinks, such as total inflow, water diversions, groundwater abstractions and recharge from precipitation during the period from 1990 to 2020. With a target significance level of 0.05, the cut-off length and the Huber's Tuning constant was set to 3 years and 2, respectively (Table 4 in Section 4.1). In addition, a Pearson correlation coefficients matrix was used to conduct the bivariate correlation analysis of the four above sources and sinks influencing groundwater storage at the significance levels of 0.01 and 0.05.

3. Results

3.1. Calibration of the groundwater flow model

Fig. 4 shows the relationship between simulated and observed hydraulic heads of all observation wells located in layers 1–3 in August 1996 and August 2014. A sharp drop in groundwater storage occurred in 2003 (Fig. 10-c in Section 3.3.1); therefore, before and after 2003 were selected to represent higher and lower steps in groundwater levels, respectively. The scattered data points for the two stress periods lie close to the diagonal line. MAE, RMSE, and R^2 were 1.967 m, 2.656 m, and 0.942 in August 1996, and 1.866 m, 2.499 m, and 0.972 in August 2014. The error, then, is acceptable given that the difference between the highest groundwater level and the lowest groundwater level in the entire basin was about 90 m. That is, after manual calibration, the calculated heads were generally consistent with the observed heads during the two typical stress periods of before and after 2003. In other words, the model effectively simulated the groundwater dynamics of the modeled aquifers and could reproduce the long-term spatial distribution of groundwater levels and the regional characteristics of the hydrogeological processes. The calibrated hydrogeological parameters are shown in Table 2.

Typical long-term observation wells in both layer 1 and layer 2 of Yinchuan City and Shizuishan City are shown in Fig. 5 and Fig. 6. Although the long-term trends in observed and computed heads are similar, seasonal fluctuations in the computed heads were smaller than the observed heads. A further decrease in storage parameters led to dry cells in the top model layer, which may be related to seasonal variations in irrigation return flow and groundwater abstractions. Furthermore, there is a large discrepancy between the observed and simulated groundwater levels. This discrepancy in the shallow aquifer can mainly

Table 2
Initial and calibrated hydraulic conductivities, specific storages and specific yields.

Materials	Initial parameters				Calibrated parameters			
	K_h (m/d)	K_v (m/d)	S_s	S_y	K_h (m/d)	K_v (m/d)	S_s	S_y
Clay	0.5	0.00100	0.00010	0.10	0.1	0.00050	0.00008	0.09
Fine sand	4.0	0.02000	0.00020	0.15	5.0	0.02564	0.00031	0.10
Coarse sand	10.0	0.20000	0.00030	0.25	10.0	0.18182	0.00033	0.11
Clay mixed with gravel	3.0	0.30000	0.00035	0.28	3.0	0.05660	0.00034	0.12
Pebble	24.0	0.60000	0.00050	0.30	30.0	0.60000	0.00036	0.20

be attributed to inaccurate estimations of irrigation return flow and canal leakage. In the confined aquifer, groundwater abstractions were obtained from annual water resources bulletins which contain large uncertainty.

3.2. Evolution of regional groundwater levels

3.2.1. Inter-annual groundwater level dynamics

The highest groundwater levels in the shallow aquifer occur in the piedmont pluvial plain in the west and the area of pluvial-alluvial fans in the south. The main groundwater flow direction is from southwest to northeast and is consistent with the change in topography. The groundwater flow direction beneath the piedmont pluvial plain and the pluvial-alluvial plain in the west is from west to east. Interannual variations in groundwater levels were not significant (Fig. 7).

The spatial distribution of groundwater levels in the deep aquifers (layers 2–3) is, overall, consistent with that in the shallow aquifer. Local differences in groundwater levels are primarily associated with concentrated areas of groundwater abstractions in Yinchuan City and Shizuishan City, which have created cones of depression (Fig. 8). In the early 1990s, such cones of depression did not exist in Shizuishan City. However, a long-term cone began to form in 1995, and with an increase in the pumping rate, the area of the cone gradually increased from 9 km^2 in the mid-1990s to 80 km^2 in 2010. After 2010, the area of the cone in Shizuishan City began to gradually decrease, and by 2020, it had returned to its size in the 1990s. Around 2006, two small cones of depression related to groundwater pumping appeared on the east side of Shizuishan City and remained stable. As for Yinchuan City, its cone of depression has gradually expanded from an area of 50 km^2 in the 1990s to five groups of smaller cones, each with an area of about 30–40 km^2 in 2020.

Where irrigation activities occur over the shallow aquifers, the seasonal variations in groundwater level were more pronounced than in the deep aquifer. Over the 30-year period, groundwater levels remained relatively stable compared to the deep aquifers. The changes in groundwater levels that did occur in layer 1 varied spatially over the area. Beneath the western piedmont pluvial plain of Yinchuan City, the groundwater levels continued to decline over the 30-year study period in the shallow aquifer (Fig. 5-a). In the eastern part of Yinchuan City, changes in groundwater levels slowed over the 30 years (Fig. 5-b, c). In the western section of Shizuishan City, groundwater levels in the shallow aquifer initially remained stable, but have declined between 2000 and 2010. After 2010, groundwater levels gradually recovered to that which existed before 2000 (Fig. 5-d, e). In the southern part of Shizuishan City, groundwater in the shallow aquifer declined slowly (Fig. 5-f).

In deep aquifers (layers 2–3) where groundwater exploitation is concentrated, the groundwater levels declined continuously, with less seasonal variation compared to the shallow aquifers. In the vicinity of the well fields west of Yinchuan City, the groundwater levels gradually recovered from 1090 m in the 1990s to 1100 m in 2020 (Fig. 6-a). North of Yinchuan City, the groundwater level declined slowly before 2005, but from 2005 to 2020, the groundwater level dropped sharply, and were superimposed on by relatively small seasonal fluctuations (Fig. 6-b). In the northeastern part of Yinchuan, groundwater levels remained stable (Fig. 6-c). The groundwater levels in the deep aquifer south of Shizuishan City declined continuously (Fig. 6-d). Within the cone of depression in the western part of Shizuishan City, the groundwater level in the deep aquifer decreased from 1990 to 2010. Since 2010, it has begun to recover to the level before 2000 (Fig. 6-e, f).

3.2.2. Seasonal groundwater level variations

The seasonal variations in groundwater levels in the shallow layer were generally higher than that in the deep aquifers. The average amplitudes of groundwater level fluctuations in the central and northern parts of the study area were about 2 m and 1.5 m, respectively. Larger amplitudes of variation (~4 m) occur in the south, most likely in response to a larger amount of irrigation, which allows significant excess irrigation return flow to infiltrate and replenish the shallow groundwater.

The annual variations in groundwater levels, water diversions (Zhao et al., 2015), the irrigation period, precipitation, and evapotranspiration are compared for Well 1–7 in Fig. 9 as an example of the changes in the shallow aquifer. The annual dynamics of the groundwater levels in the irrigated area are significantly affected by the irrigation activities and water diversion processes. For example, seasonal fluctuations in groundwater levels in the shallow aquifer are temporally consistent with the cycle of irrigation and water diversions from the Yellow River, and can be subdivided into four stages: 1) a period of no irrigation that occurs before the beginning of spring irrigation (December to March); the groundwater is at the lowest levels; 2) a period of irrigation, which begins with the onset of water diversions in late April, at which time groundwater levels begin to rise. The amount of water diverted from the Yellow River increases in May and August, resulting in the highest groundwater levels which correspond to a period of maximum irrigation; 3) an intermittent period of irrigation in late September and late

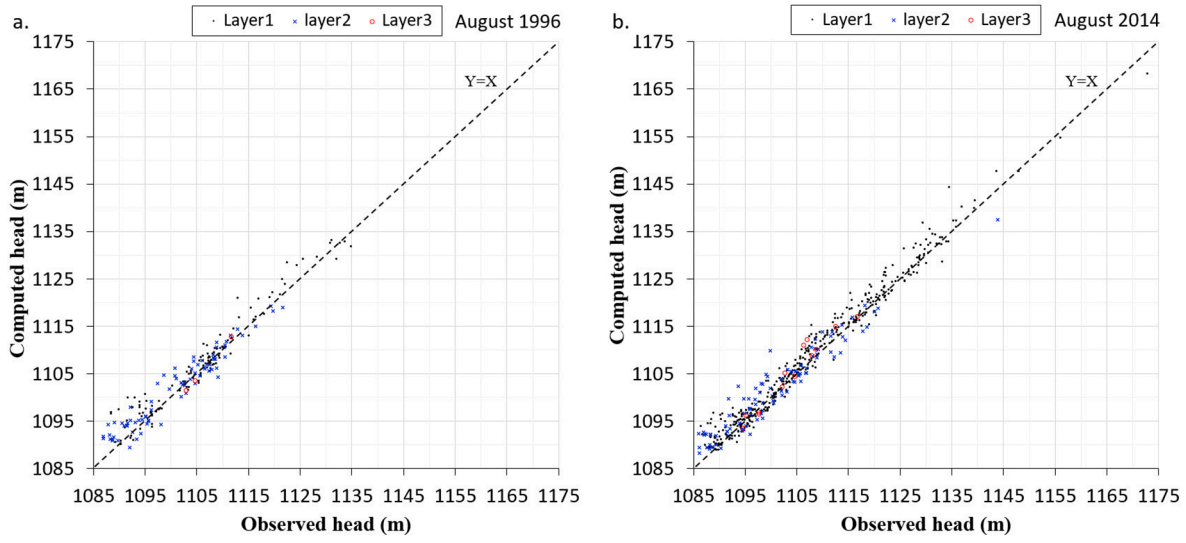

Fig. 4. Scatter plots of observed versus computed hydraulic heads: a) in Aug. 1996; b) in Aug. 2014.

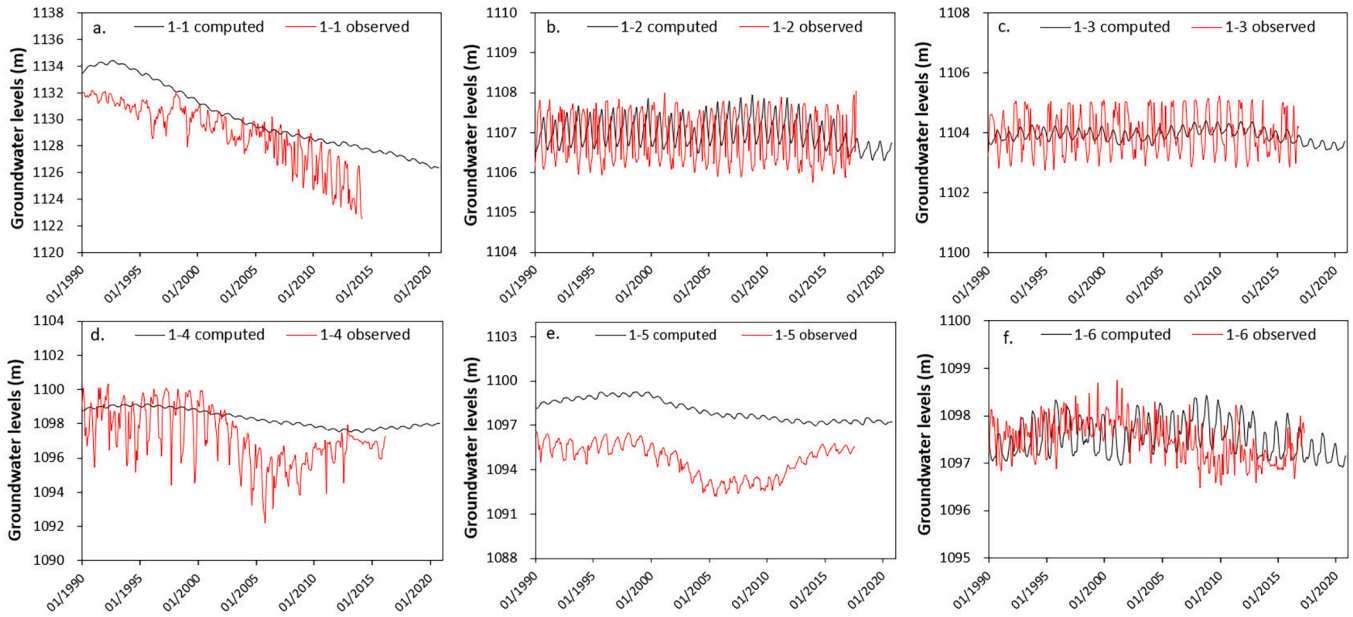

Fig. 5. Fitting curves of computed heads (black) to observed heads (red) at typical observation wells in layer 1; a) Well 1–1 in Yinchuan; b) Well 1–2 in Yinchuan; c) Well 1–3 in Yinchuan; d) Well 1–4 in Shizuishan; e) Well 1–5 in Shizuishan; f) Well 1–6 in Shizuishan. (For interpretation of the references to colour in this figure legend, the reader is referred to the web version of this article.)

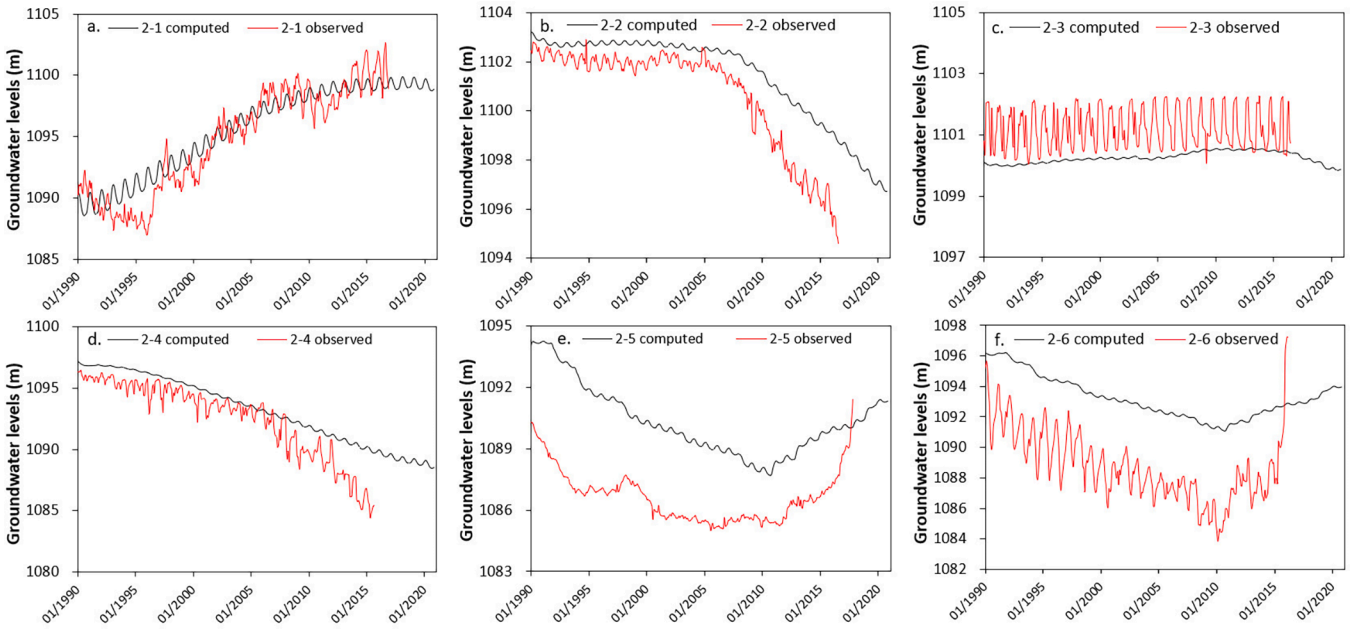

Fig. 6. Fitting curves of computed heads (black) to observed heads (red) at typical observation wells in layer 2; a) Well 2–1 in Yinchuan; b) Well 2–2 in Yinchuan; c) Well 2–3 in Yinchuan; d) Well 2–4 in Shizuishan; e) Well 2–5 in Shizuishan; f) Well 2–6 in Shizuishan. (For interpretation of the references to colour in this figure legend, the reader is referred to the web version of this article.)

October, during which the amount of water diversions from the Yellow River decreases, and groundwater levels begin to drop; and 4) a period of winter irrigation extending from late October to late November. Winter irrigation is carried out for soil salt leaching and moisture storage. The groundwater level rises again to a level similar to that during the irrigation period.

Of the four factors discussed above, the correlation between the groundwater levels and water diversions is strongest with a correlation coefficient of 0.928, which is significant at the 0.01 level (Table 3). Climate factors show moderate correlation with groundwater levels and water diversions, and are significant at the 0.05 and 0.01 level, respectively. Recharge from precipitation may contribute to higher groundwater levels during the rainy season. However, relatively high evapotranspiration should result in lower groundwater levels. Therefore, climate factors have less effect on groundwater levels.

The seasonal fluctuations in groundwater levels exhibited the same pattern throughout the study area; however, the amplitude of the groundwater level fluctuations varied spatially. This spatial variation

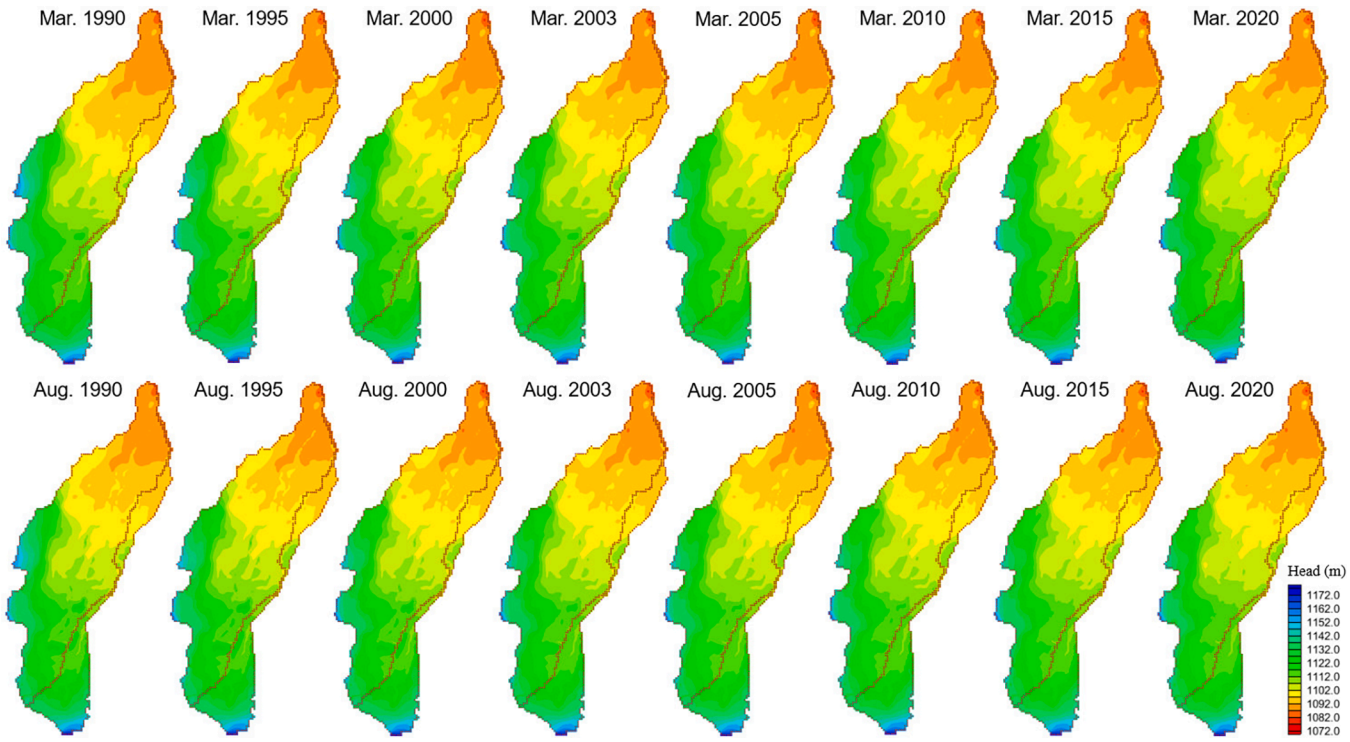

Fig. 7. Shaded groundwater level contour map of layer 1 in March and August 1990, 1995, 2000, 2003, 2005, 2010, 2015 and 2020.

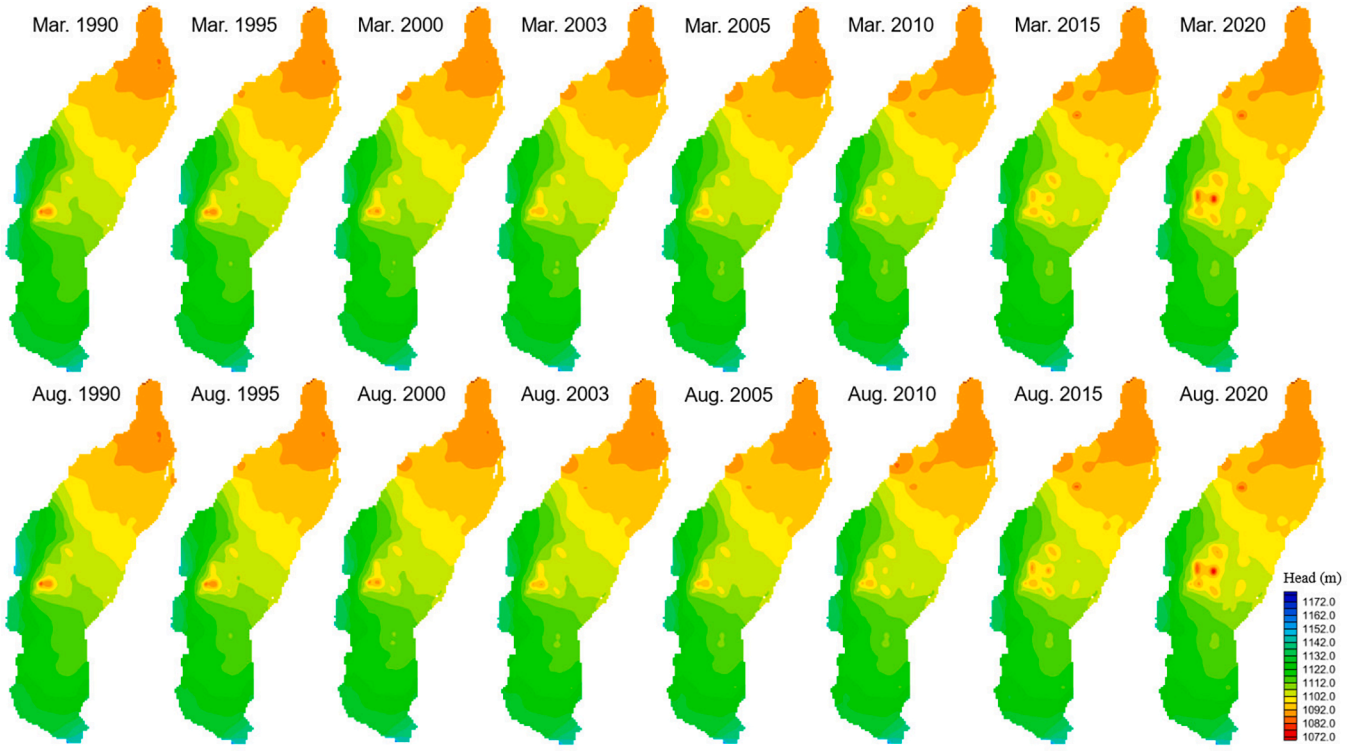

Fig. 8. Shaded groundwater level contour map of layer 2 in March and August 1990, 1995, 2000, 2003, 2005, 2010, 2015 and 2020.

was mainly attributable to recharge and hydrogeological conditions and could be subdivide into specific areas including: 1) the alluvial-lacustrine plain, where irrigation is widespread. The intra-annual dynamics of the shallow groundwater levels are mainly affected by irrigation and water diversions in the central and southern part of the basin, and levels are dependent on irrigation. The amplitude of the groundwater fluctuations is relatively large. 2) An area in the northern part of the catchment where downstream irrigation occurs and the amplitude of the changes in groundwater levels are relatively low. Due to the shallow depth of groundwater in the northern region, the amount of evapotranspiration is large. 3) In areas of non-agricultural irrigation, such as in the piedmont pluvial plain and urban areas, the magnitude of

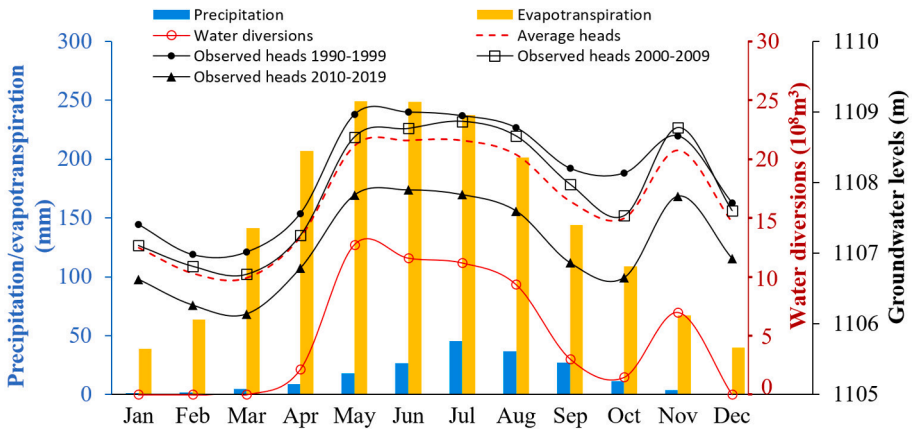

Fig. 9. Variations in intra-annual groundwater levels observed in Well 1–7 in the Yinchuan area, along with the 30-year monthly average precipitation, evapotranspiration, and water diversions from 1990 to 2019.

the groundwater level fluctuations in the shallow aquifer is small. In the piedmont area, the groundwater level is deep and evapotranspiration is small. In addition, a large transmissivity and hydraulic gradient primarily generate horizonal flow, so seasonal variations in groundwater levels are small. In urban areas, land cover is often impermeable, limiting precipitation infiltration. Thus, the fluctuations in groundwater levels are also small. 4) The groundwater level dynamics in most areas with deep aquifers exhibit relatively small interannual and seasonal fluctuations. However, in areas of concentrated pumping (Yinchuan City and Shizuishan City), the groundwater levels vary with pumping rates.

3.3. Groundwater budget

3.3.1. Water budget components and change in groundwater storage

The simulated groundwater budget for the period between 1990 and 2020 (Table S3, Fig. 10-a) shows that recharge from irrigation return flow and canal leakage is the main inflow component to the groundwater system, accounting for about 70% of the total recharge. The other inflow components include lateral flow from the western border and recharge from precipitation. Major groundwater outflows include groundwater withdrawals from shallow and deep aquifers, evapotranspiration, and drain discharges, which collectively account for approximately 90% of the total outflows.

From 1990 to 1999, the annual amount of water diverted from the Yellow River increased steadily in riparian provinces. As a result, discharge in the Yellow River was significantly reduced. To alleviate severe shortages in water resources, the Yellow River Water Conservancy Commission officially launched a unified scheduling program of water diversions from the Yellow River in March 1999. Since 2000, the amount of water diversion from the Yellow River has strictly followed water allocation regulations, and the diversion of water from the river has started to decline (Fig. 10-b). The inflow of water from the upper reaches of the Yellow River reached its lowest value in 2003, a dry year, which led to a sharp decline in water diversions. Since 2004, the rate of decline has slowed.

Recharge of the groundwater system and water diversions are highly correlated (see Section 4.1). The trend, visible in the time series of total inflow, is mainly associated with the variability in irrigation return flow recharge and canal leakage. Lateral inflow from the western boundary along the Helan Mountains has been relatively stable. Groundwater abstractions increased in the periods of lower water diversions (Fig. 10-a, b). Water diversions dropped dramatically in 2003 and reached another low after 2016. Conversely, groundwater abstractions increased during these two periods.

Groundwater outflows were largely dependent on inflows, and overall trends and fluctuations between the two were similar. The relation between the two is probably related to the dense distribution of drains in the Yinchuan Basin and the use of traditional modes of irrigation that involves large-scale water spreading and large drainages. The discharge from these drains accounts for a large proportion of the total outflow and is consistent with trends in water diversions (Fig. 10-b). Within a given year, the discharge from drains was proportional to the irrigation water use.

Since 2000, groundwater storage has declined significantly; that is, the total outflow is greater than the total inflow (Fig. 10-c). The cumulative depletion in storage has continuously increased during the 30-year study period. Since 2014, the depletion in groundwater storage has become even more rapid. By 2020, the depletion in groundwater storage had reached 1.89×10^9 m^3.

3.3.2. Water exchange between groundwater and surface water

Over the entire basin, discharge of groundwater to the Yellow River is greater than the recharge of groundwater from the Yellow River (Fig. 11). The continuous increase in irrigation between 1990 and 2000 increased groundwater levels in most parts of the study area, and gradually increased the discharge of groundwater to the Yellow River. After 2000, with the gradual reduction in irrigation water, the discharge of groundwater to the Yellow River gradually decreased. The amount of groundwater recharge from the Yellow River was relatively stable before 2017. After 2017, the increase in groundwater abstractions and the lowering of the groundwater levels led to an increase in groundwater recharge from the Yellow River.

Table 3
Pearson correlation coefficients between total inflow and the three main budget items at Well 1–7.

Budget items	Groundwater levels	Water diversions	Evapotranspiration	Recharge from precipitation
Groundwater levels	1.000			
Water diversions	0.928**	1.000		
Evapotranspiration	0.591*	0.779**	1.000	
Recharge from precipitation	0.692*	0.728**	0.750**	1.000

** Significance level = 0.01.
* Significance level = 0.05.

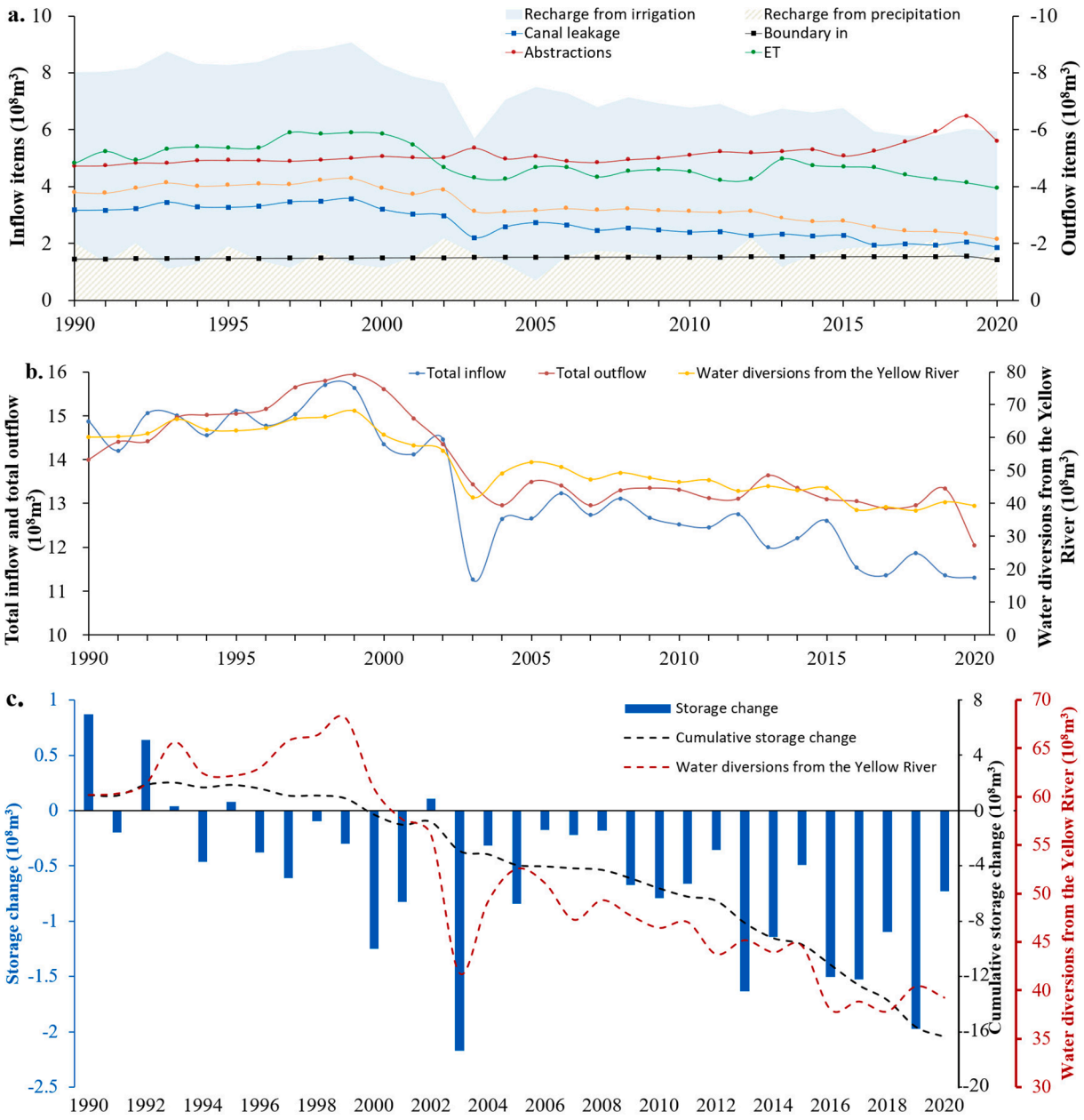

Fig. 10. Temporal change in budget items in the Yinchuan Basin from 1990 to 2020; a) annual inflow and outflow components; annual water diversion from the Yellow River (data from NWRD 2000-2020 and Zhao 2015); b) total inflow and outflow; c) storage change. (For interpretation of the references to colour in this figure legend, the reader is referred to the web version of this article.)

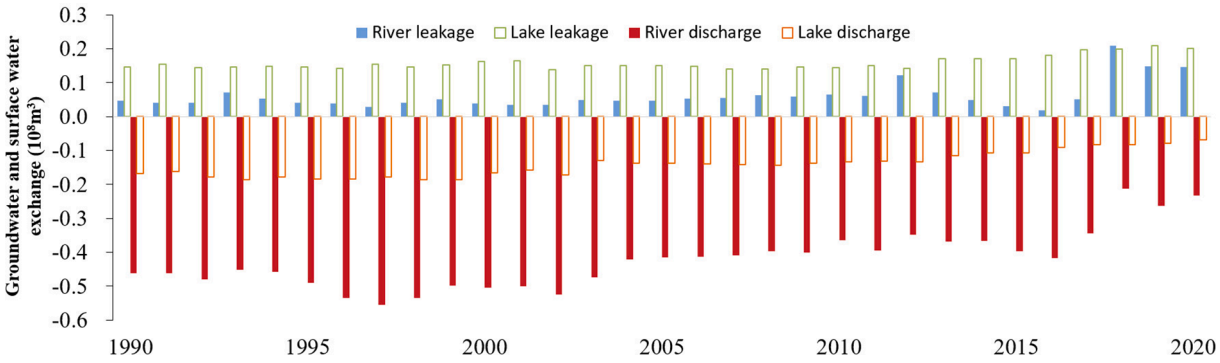

Fig. 11. Water exchange between groundwater and surface water.

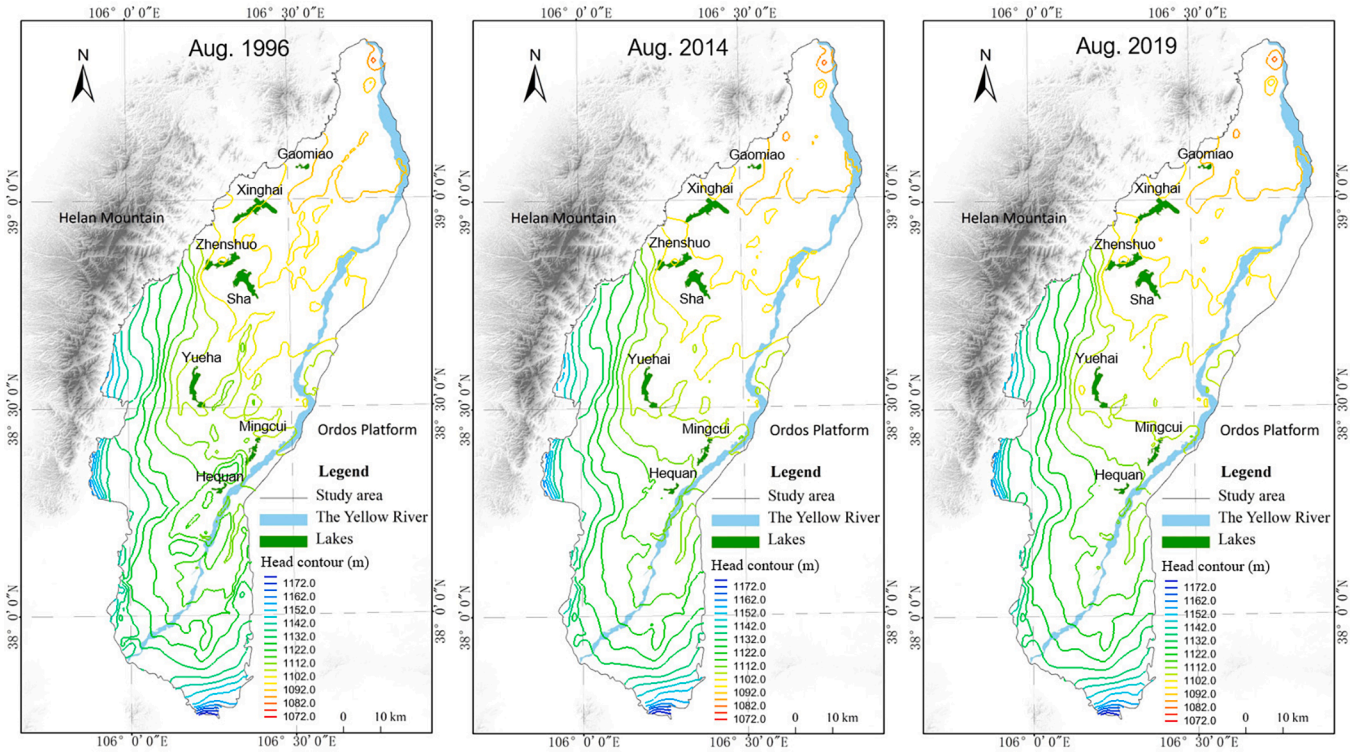

Fig. 12. Lakes identified as flow-through lakes in the unconfined aquifer.

The discharge of groundwater to lakes is lower than the recharge of groundwater from lakes. Lakes in the Yinchuan Basin simultaneously receive groundwater inflow from one portion of the shoreline and recharge the groundwater system along the other; therefore, all lakes are flow-through lakes (Fig. 12). The largest amount of groundwater recharge is from Mingcui Lake located in the eastern part of Yinchuan City. Since 2012, outflow to groundwater from all of these lakes except Sha Lake and Gaomiao Lake have substantially increased (Fig. 13-a). The increased outflow to groundwater near these lakes is related to the increase in groundwater abstractions near these lakes and the establishment of several new well fields in the eastern part of Yinchuan City. The water levels of the lakes are maintained through water diversions from the canals. As the difference between lake level and the groundwater level increases, groundwater recharge by these lakes increases. Due to the relatively low groundwater abstractions near Xinghai Lake, Gaomiao Lake and Sha Lake, the groundwater recharge from these three lakes remained relatively stable. The amount of discharge from groundwater to Mingcui Lake,Yuehai Lake and Sha Lake decreased over

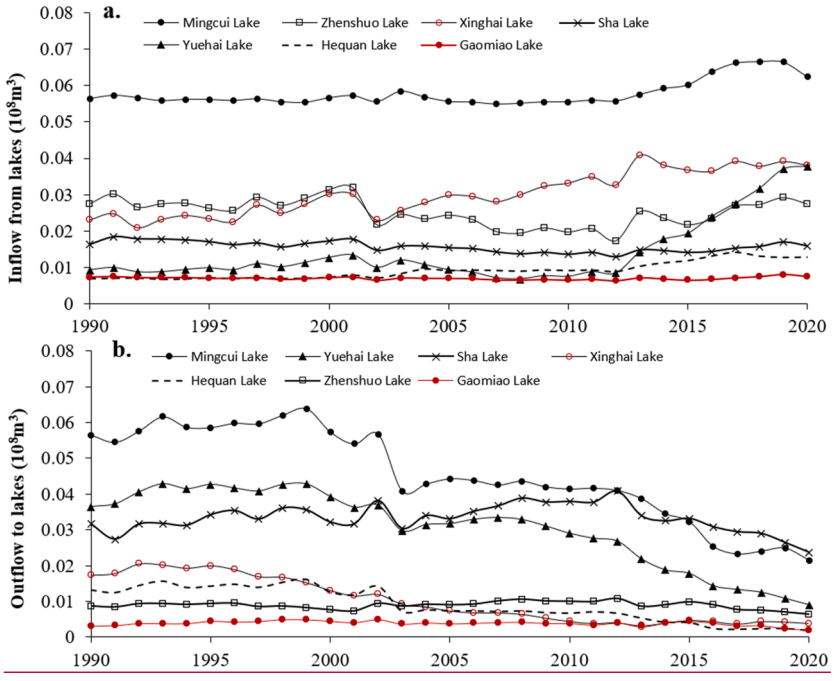

Fig. 13. Water exchange between lakes and groundwater; a) inflow; b) outflow.

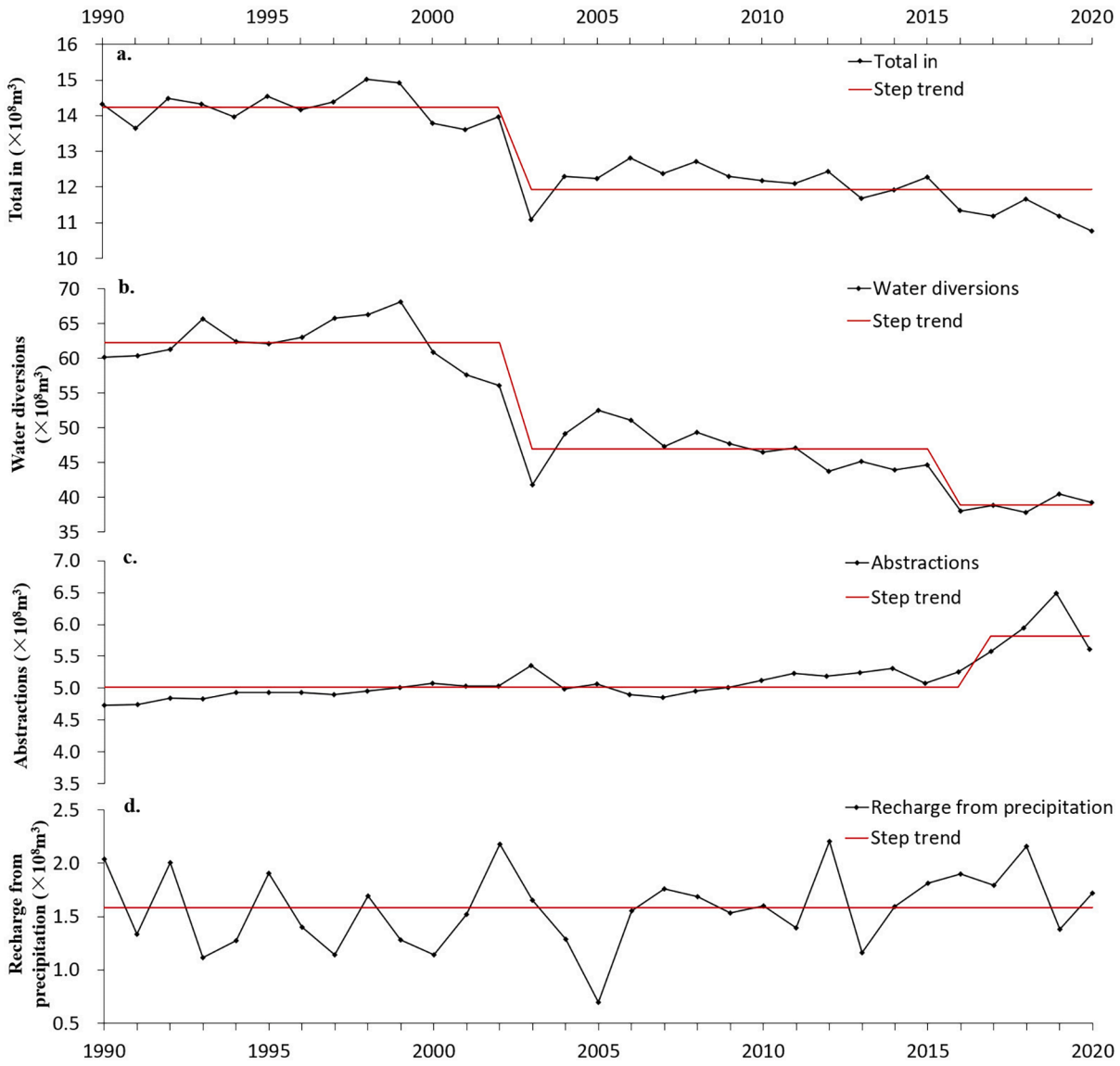

Fig. 14. Regime shift detection results with a cut-off value of 3 years for: a) total inflow, b) water diversions, c) abstractions (data from NWRD 2000-2020) and d) recharge from precipitation.

Table 4
Statistics of the regime shift detection analysis.

Budget items	significance level	Cut-off length	Huber's Tuning constant	Year of shifts		Mean (10^8 m^3/a)		
				1st Shift	2nd Shift	Step1	Step 2	Step 3
Total inflow	0.05	3	2	2003	/	14.24	11.92	/
Water diversions	0.05	3	2	2003	2016	62.80	47.57	38.89
Abstractions	0.05	3	2	/	2017	/	5.02	5.91
Recharge from precipitation	0.05	3	2	/	/	1.58	/	/

the study period. The discharge from groundwater to the rest of the four lakes remained relatively stable (Fig. 13-b).

Compared with the overall groundwater budget of the Yinchuan Basin, the amount of groundwater-surface water exchange is small. However, these groundwater and surface water interactions have significant environmental consequences. For example, the gradual reduction of groundwater recharge and the increase in groundwater abstractions may result in lake leakage, which in turn can lead to a shrinkage in lake area or even dry lakes. To maintain the area and the ecological conditions of the lakes, water diversions are required to maintain lake water levels, in particular in Mingcui Lake, Xinghai Lake and Yuehai Lake.

4. Discussion

4.1. The causes of stepped trend in the groundwater budget

Water diversions, groundwater abstractions, and recharge from precipitation were analyzed by regime shift analysis and correlation analysis as potential factors controlling the temporal changes in

Table 5
Pearson correlation coefficients between total inflow and the three main budget items.

Budget items	Total inflow	Water diversions	Abstractions	Recharge from precipitation
Total inflow	1.000			
Water diversions	0.965**	1.000		
Abstractions	−0.463**	−0.428*	1.000	
Recharge from precipitation	−0.079	−0.314	0.019	1.000

** Significance level = 0.01.
* Significance level = 0.05.

groundwater resources. The temporal trends in irrigation return flow and canal leakage were similar to the water diversions from the Yellow River. Therefore, this study analyzed the effect of agricultural irrigation activities on groundwater recharge on the basis of the water diversions from the Yellow River (rather than irrigation return flow and canal leakage). The trend in the mean total annual inflow abruptly dropped in 2003 (Fig. 14-a). The average values of the steps before 2003 and after 2003 were 14.24×10^8 m^3/a and 11.92×10^8 m^3/a, respectively (Table 4). Before 2003, water diversions exhibited a similarly high value which abruptly changed in 2003 (Fig. 14-b). That is, the reduction in total inflow and groundwater storage from 1990 to 2016 was dominated by a decline in available water diversions from the Yellow River (Fig. 14-a, b). In contrast to the trend in total inflow, the step trend of water diversions showed another sharp drop in 2016. In other words, a three-step trend was identified, where the average values of each step are 62.29×10^8 m^3/a, 46.92×10^8 m^3/a, and 38.89×10^8 m^3/a. The groundwater abstractions for agriculture exhibit a two-step trend; the shift point occurs in 2017. The average abstraction volumes during the two periods were $5.02\times10^8/a$ m^3 (before 2017) and 5.91×10^8 m^3/a (after 2017). We hypothesize that groundwater abstractions were increased from 2017 (Fig. 14-c) to compensate for a shortage in water demand that resulted from the reduction in water diversions from the Yellow River since 2016 (Fig. 14-b). As a result, the drop of total inflow from 2016 (Fig. 14-a) was not significant. In combination, the trends show that water diversions from the Yellow River have had a decisive impact on the total inflow. The impact of total inflow since 2016 is collectively determined by water diversions and groundwater abstractions. Most of the precipitation in the Yinchuan Basin is concentrated from May to September. Regime shift detection was unable to identify step trends in precipitation infiltration during the study period (Fig. 14-d), suggesting that the long-term trend in total inflow was not significantly affected by recharge from precipitation.

A bivariate correlation analysis was used to calculate the correlation coefficients among total inflow, water diversions, abstractions, and recharge from precipitation (Table 5). The Pearson correlation coefficient between total inflow and water diversion is 0.965 (a strong correlation), which is significant at the 0.01 level. The correlation suggests that water diversion is a decisive factor controlling groundwater recharge. The Pearson correlation coefficient between abstractions and water diversions is −0.428, which is significant at the 0.05 level. When water diversions decrease, groundwater abstractions increase to meet water demands. However, recharge from precipitation does not exhibit a significant correlation with total inflow, water diversions or abstractions at a significance level of 0.05. This is presumably because recharge from precipitation only affects the short-term interannual fluctuations of total inflow, which mainly reflects the difference between precipitation recharge in wet and dry years. Water diversions are mainly policy-

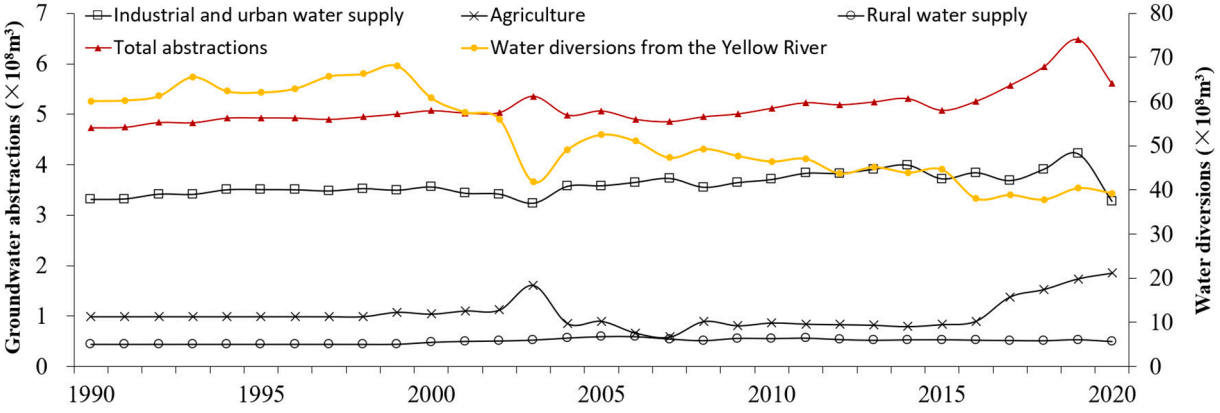

Fig. 15. Temporal change in annual groundwater abstractions by different users in the Yinchuan Basin from 1990 to 2020.

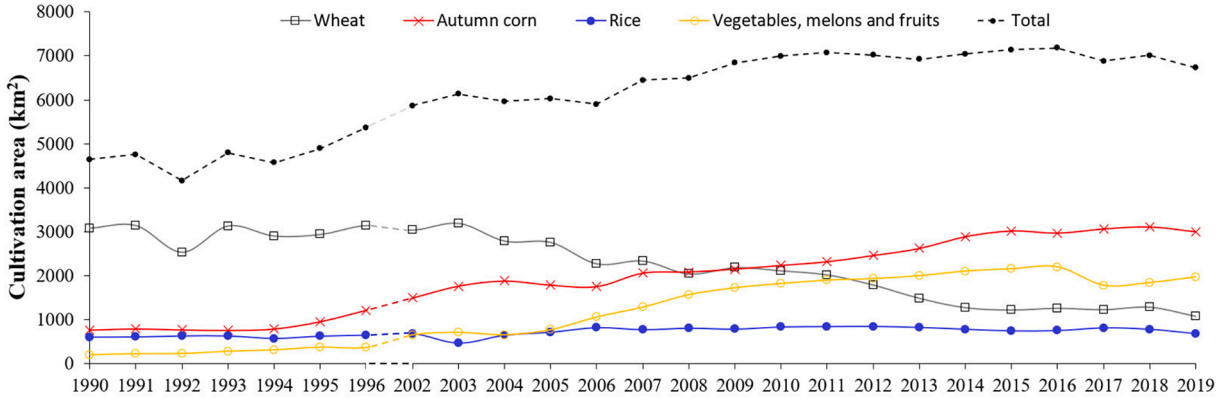

Fig. 16. Changes in the cultivation area of major crops in the Yinchuan Basin from 1990 to 2019.

controlled; thus, diversions are only weakly correlated with recharge from precipitation.

4.2. Adaptation for a reduction in river water diversions

With increased urbanization between 1990 and 1999, the consumption of water for domestic needs and industrial activities have increased significantly, along with the use of water for irrigation. The amount of total groundwater abstractions and the amount of water diverted from the Yellow River increased simultaneously. The implementation of the National Western Development Strategy in 2000 led to an increase in both population and water demand. Since then, the gradual reductions in water diversions have not been sufficient to meet the growing water demand (Fig. 15). Total groundwater abstractions has been slowly growing to deal with the shortage of water resources caused by the reduction of water diversions from the Yellow River. In 2003 and during 2016-2020, the amount of water taken from the Yellow River reached its lowest value. As a result, there were sharp increases in groundwater abstractions in these particular years.

Groundwater abstractions by different users showed different trends. The relatively low groundwater abstractions for rural water supplies remained stable for 30 consecutive years. Groundwater abstracted from centralized well fields for industrial and urban water supplies accounted for the largest proportion of total abstractions, which is in line with the growth in total abstractions. With the exception of 2003, urban and industrial water use was restricted by the sharp drop in water diversions. The abstractions of groundwater for agriculture remained stable before 2003, but to compensate for the shortage in agricultural water caused by the sharp drops in river water diversions in 2003 and during 2016–2020, groundwater abstractions for agriculture increased sharply (Fig. 15). Therefore, an indirect (inverse) relationship exists between the agricultural abstractions of groundwater and the water diversions from the river (Fig. 10-b, c; Fig. 15). It is worth noting that after 2004, the amount of water diverted from the Yellow River decreased, but agricultural abstractions did not increase significantly. We speculate that after the unified regulation of water diversion from the Yellow River in 2000 and the extreme drought year in 2003, the Yinchuan Basin began to implement large-scale crop pattern adjustments and agricultural water-saving measures to reduce the agricultural water demand.

Water-saving irrigation projects have been carried out since 2000. For example, the crop pattern for the entire Ningxia region was adjusted (NSB, 1991-2020), resulting in a reduction in summer grain crops (e.g., wheat) and an increase in autumn grain crops (e.g., corn). These changes in crop patterns reduce irrigation water requirements (Fig. 16). Farmers have also 1) reduced the planting area of crops with high water consumption and low efficiency (e.g., wheat), 2) maintained the planting area of rice, and 3) developed water-saving irrigation for rice cultivation. Moreover, farmers have expanded the area of crops with lower water consumption, including drought-tolerant crops (e.g., autumn corn, forage grass, and herbs) and crops using water-saving irrigation techniques (e.g., vegetables, melons, and fruits). The total cultivation area increased before 2010 and remained stable after 2010. In addition, water-saving irrigation techniques have been improved. For example, the irrigation of wheat and corn was changed from flood irrigation to furrow irrigation. Micro-irrigation has also been developed for vegetables, melons, and fruits, and sprinkler irrigation has been developed for forage grass. At present, the leakage of water from the canal system accounts for a large proportion of water loss. In the future, the water diversions of the Yellow River will continue to decrease. We therefore suggest that the anti-leakage treatment of the canal system should be further strengthened, and the main canals combined to reduce the leakage losses of water during its delivery to agricultural fields.

4.3. Limitations

There are a number of limitations to the model developed in this study. First, hydrogeological parameters (e.g., K and S_s) vary with depth. However, the values of each hydrogeological parameter in each lithology (geological unit) were assigned uniformly by the HUF package for the differing depths considered in this model. In addition, there is a lack of hydrogeological parameter data for the deep aquifer materials (depths greater than 300 m). Thus, we assumed that the values of the hydrogeological parameters of the lithologic units at different depths are the same. Second, the depths of long-term groundwater level observations available for model calibration are limited, and most observations were at depths of less than 300 m. Third, the model was constructed for monthly stress periods, while the actual data were collected on an annual scale. The seasonal variations of each item (e.g., recharge from irrigation return flow, canal leakage) were based on the proportion of water diversions in different months (Zhao et al., 2015), which may result in uncertainties in the seasonal fluctuations of the computed heads. Fourth, because maps of crop patterns for different years are not available, the zonation of irrigation return flow was conducted according to the administrative division, land-use, and soil type. In addition, the infiltration coefficient of irrigation water in different years was assumed to be a fixed value within the same zone, as was the effective utilization coefficient. Fifth, since data describing the degree to which the canals were lined in different years were not available, the leakage coefficient of the canals in different years was assumed to be a fixed value within the same zone, as was the effective utilization coefficient. Sixth, due to the lack of hydrogeological boreholes in the piedmont of the Helan Mountains, the lateral recharge along the piedmont boundary was assumed on the basis of the hydraulic gradient between the boreholes in the front of the alluvial fans. The above limitations have presumably led to uncertainty in parameter calibration and bias in the model results. To address all the limitations mentioned, investigations will be conducted in the future to improve the model, thereby increasing its ability to assess the mechanisms of deep groundwater flow dynamics and the prediction of future changes in the groundwater system. Despite these limitations, our present results provided general patterns of groundwater flow dynamics under the effects of human activities and climate change.

5. Conclusions

Changes in the environment have profound effects on the evolution of hydrogeological processes, especially in arid and semi-arid regions. Documenting the response of a regional groundwater system to human activities and climate change is a challenge. A long-term transient groundwater flow model can be used to reconstruct historical changes in hydrogeological processes and quantify the interaction between groundwater and surface water systems. The main conclusions from this study are as follows: 1) groundwater storage was continuously depleted over the 30-year (1990–2020) study period, reaching a cumulative depletion of 1.89×10^9 m^3. Irrigation return flow and canal leakage were the main sources of recharge to the groundwater system. The main groundwater outflows included groundwater abstractions, drain discharge, and evapotranspiration. 2) Hydrogeological processes were mainly affected by human activities in the Yinchuan Basin. Human activities (particularly water diversions from the Yellow River) dominated the long-term trend in groundwater storage. Climate only affected short-term interannual fluctuations in groundwater storage. 3) In most years, the computed groundwater budget shows that recharge from surface water to groundwater was lower than that from groundwater to surface water. The continuous decline in groundwater levels during the 30-year study period led to an increase in the amount of groundwater recharge from the Yellow River and lakes. Conversely, the amount of groundwater discharged to the Yellow River and lakes has continued to decrease. There is an increasing requirement for artificially supplied water to lakes to maintain their water levels. 4) Water diversions from the Yellow River has dropped since 2000, resulting in a continuous reduction in groundwater recharge and storage. The amount of

groundwater abstractions increased when water diversions from the Yellow River were insufficient to meet the water demand. Water-saving irrigation and adjustments to the crop pattern were implemented to reduce the requirements for irrigation.

In the Yinchuan Basin, a representative arid and semi-arid area of northern China, groundwater is being depleted and the ongoing development is not sustainable. Groundwater resources are more vulnerable to policy changes pertaining to water diversions and land use change than climate factors. The risk of future groundwater depletion may likely come from human impacts, such as policies governing surface water diversions and groundwater abstraction intensity. This study not only documented the temporal and spatial variations in groundwater levels in a typical arid and semi-arid area of northwest China, but also evaluated the impact of human activities on the groundwater system. The dynamic response in groundwater levels, irrigation patterns, and groundwater abstractions to the change in water diversions from the Yellow River was evident. The results will enable water managers to predict future changes in groundwater levels and storage caused by changes in land use and water diversions through scenario analysis. It can also provide insights for creating sustainable management plans in other arid and semi-arid regions.

CRediT authorship contribution statement

Jie Li: Data curation, Writing – original draft, Writing – review & editing. **Yangxiao Zhou:** Funding acquisition, Supervision, Writing – review & editing. **Wenke Wang:** Funding acquisition, Supervision, Writing – review & editing. **Sida Liu:** Writing – review & editing. **Ying Li:** Data curation, Investigation. **Ping Wu:** Data curation, Investigation.

Declaration of Competing Interest

The authors declare that they have no known competing financial interests or personal relationships that could have appeared to influence the work reported in this paper.

Data availability

The authors do not have permission to share data.

Acknowledgment

This study was funded by the National Natural Science Foundation of China (Grant No. 42130710), the Natural Science Basic Research Program of Shaanxi Province (Grant No. 2021JCW-16), and the “The Investigation and Evaluation on the Development and Utilization of Groundwater Resources and the Effect of Ecological Environment Protection Along the Yellow Ecological Economic Zone” Project of the Ningxia Finance Department (Grant No. 6400201901273). The first author is grateful to the China Scholarship Council (No. 202006560048). We are thankful for the technical support by Prof. Fusheng Hu from China University of Geosciences (Beijing) and Dr. Feilong Jie from Xi’an University of Technology. The authors are grateful to the editors and two anonymous reviewers for their valuable comments and suggestions which helped to improve the manuscript.

Appendix A. Supplementary data

Supplementary data to this article can be found online at https://doi.org/10.1016/j.jhydrol.2022.128619.

References

Anderman, E.R., Hill, M.C., 2000. MODFLOW-2000, the U.S. Geological Survey Modular Ground-Water Model -Documentation of the Hydrogeologic-Unit Flow (HUF) Package. 2000-342, Denver, CO. DOI:10.3133/ofr00342.

Aquaveo, 2017. GMS User’s Manual 10.3. Retrived from http://gmsdocs.aquaveo.com/GMS_User_Manual_v10.3.pdf.

Burns, E.R., Bentley, L.R., Therrien, R., Deutsch, C.V., 2010. Upscaling facies models to preserve connectivity of designated facies. Hydrogeol. J. 18 (6), 1357–1373.

Carlson, M.A., Lohse, K.A., McIntosh, J.C., McLain, J.E.T., 2011. Impacts of urbanization on groundwater quality and recharge in a semi-arid alluvial basin. J. Hydrol. 409 (1-2), 196–211.

CGS, 2012. Handbook of Hydrogeology. 2nd Edition (in Chinese). China Geological Survey (CGS). Geological Press.

Feng, D., Zheng, Y.i., Mao, Y., Zhang, A., Wu, B., Li, J., Tian, Y., Wu, X., 2018. An integrated hydrological modeling approach for detection and attribution of climatic and human impacts on coastal water resources. J. Hydrol. 557, 305–320.

Friend, P.F., 1983. Towards the Field Classification of Alluvial Architecture or Sequence, Modern and Ancient Fluvial Systems. In: Collinson, J.D., Lewin, J. (Eds.), Modern and Ancient Fluvial Systems. Blackwell Publishing Ltd., Oxford, UK, pp. 345–354.

Fu, G., Crosbie, R.S., Barron, O., Charles, S.P., Dawes, W., Shi, X., Van Niel, T., Li, C., 2019. Attributing variations of temporal and spatial groundwater recharge: A statistical analysis of climatic and non-climatic factors. J. Hydrol. 568, 816–834.

Gibling, M.R., 2006. Width and thickness of fluvial channel bodies and valley fills in the geological record: a literature compilation and classification. J. Sediment. Res. 76 (5), 731–770. https://doi.org/10.2110/jsr.2006.060.

GSIN, 2016. Hydrogeological and Environmental Geological Survey Report of Ningxia Yellow River Economic Belt.

Han, S., Zhang, F., Zhang, H., An, Y., Wang, Y., Wu, X.i., Wang, C., 2013. Spatial and temporal patterns of groundwater arsenic in shallow and deep groundwater of Yinchuan Plain, China. J. Geochem. Explor. 135, 71–78.

Harbaugh, A.W., Langevin, C.D., Hughes, J.D. et al., 2017. MODFLOW-2005 version 1.12.00, the U.S. Geological Survey modular groundwater model: U.S. Geological Survey Software Release, 03 February 2017. DOI:10.5066/F7RF5S7G.

Harbaugh, A.W., 2005. MODFLOW-2005, the U.S. Geological Survey modular ground-water model – the Ground-Water Flow Process: U.S. Geological Survey Techniques and Methods. 6-A16. DOI:10.3133/tm6A16.

Hou, X., Wang, W., Wang, Z., Ma, Z., Guan, C., Xi, D., Li, P., Li, J., Huang, X., 2022. Hydrogeological Processes and Hydrochemical Effects in the Manas River Catchment, Northwest China, over the Past 60 Years. J. Hydrol. 614, 128338.

Jimenez-Martinez, J., Candela, L., Molinero, J., Tamoh, K., 2010. Groundwater recharge in irrigated semi-arid areas: quantitative hydrological modelling and sensitivity analysis. Hydrogeol. J. 18 (8), 1811–1824.

Jyrkama, M.I., Sykes, J.F., 2007. The impact of climate change on spatially varying groundwater recharge in the grand river watershed (Ontario). J. Hydrol. 338 (3), 237–250. https://doi.org/10.1016/j.jhydrol.2007.02.036.

Hill, M.C., Banta, E.R., Harbaugh, A.W. et al., 2000. MODFLOW-2000, the U.S. Geological Survey modular ground-water model; user guide to the observation, sensitivity, and parameter-estimation processes and three post-processing programs. 2000-184, Denver, CO. DOI:10.3133/ofr00184.

Langevin, C.D., Thorne Jr, D.T., Dausman, A.M. et al., 2008. SEAWAT Version 4: A Computer Program for Simulation of Multi-Species Solute and Heat Transport. 6-A22. DOI:10.3133/tm6A22.

Li, H., Lu, Y., Zheng, C. et al., 2020a. Seasonal and inter-annual variability of groundwater and their responses to climate change and human activities in arid and desert areas: a case study in Yaoba Oasis, Northwest China. Water, 12(1). DOI: 10.3390/w12010303.

Li, J., Wang, W., Cheng, D., Li, Y., Wu, P., Huang, X., 2021. Hydrogeological structure modelling based on an integrated approach using multi-source data. J. Hydrol. 600, 126435.

Li, X.Y., Wu, H., Qian, H., 2020b. Groundwater contamination risk assessment using intrinsic vulnerability, pollution loading and groundwater value: a case study in Yinchuan plain, China. Environ. Sci. Pollut. Res. 27 (36), 45591–45604. https://doi.org/10.1007/s11356-020-10221-4.

Liu, S., Zhou, Y., Luo, W., et al., 2022. A numerical assessment on the managed aquifer recharge to achieve sustainable groundwater development in Chaobai River area, Beijing, China. J. Hydrol. 613, 128392 https://doi.org/10.1016/j.jhydrol.2022.128392.

Liu, S., Zhou, Y., Tang, C., McClain, M., Wang, X.-S., 2021. Assessment of alternative groundwater flow models for Beijing Plain. China. J. Hydrol. 596, 126065.

Ma, Z., Wang, W., Zhao, M., Hou, X., Wang, Z., Zheng, H., 2022. Non-Darcy flow through a natural streambed in a disconnected stream. Water Resour. Res. 58 (3) https://doi.org/10.1029/2021wr031356.

Meixner, T., Manning, A.H., Stonestrom, D.A., Allen, D.M., Ajami, H., Blasch, K.W., Brookfield, A.E., Castro, C.L., Clark, J.F., Gochis, D.J., Flint, A.L., Neff, K.L., Niraula, R., Rodell, M., Scanlon, B.R., Singha, K., Walvoord, M.A., 2016. Implications of projected climate change for groundwater recharge in the western United States. J. Hydrol. 534, 124–138.

Mi, L., Tian, J., Si, J., Chen, Y., Li, Y., Wang, X., 2020. Evolution of groundwater in Yinchuan oasis at the upper reaches of the Yellow River after water-saving transformation and its driving factors. Int. J. Environ. Res. Public Health 17 (4), 1304.

Miall, A.D., 2006. Reconstructing the architecture and sequence stratigraphy of the preserved fluvial record as a tool for reservoir development: a reality check. AAPG Bull. 90 (7), 989–1002. https://doi.org/10.1306/02220605065.

Nofal, S., Travi, Y., Cognard-Plancq, A.-L., Marc, V., 2019. Impact of infiltrating irrigation and surface water on a Mediterranean alluvial aquifer in France using stable isotopes and hydrochemistry, in the context of urbanization and climate change. Hydrogeol. J. 27 (6), 2211–2229.

NSB, 1991-2020. Statistical yearbook of Ningxia (in Chinese), Ningxia Statistical Bureau and Ningxia Survey Team of the National Bureau of Statistics (NSB), Yinchuan, China.

NWRD, 2000-2020. Ningxia Water Resources Bulletin (in Chinese), Ningxia Water Resources Department (NWRD), Yinchuan, China.

Pulido-Velazquez, M., Peña-Haro, S., García-Prats, A., Mocholi-Almudever, A.F., Henriquez-Dole, L., Macian-Sorribes, H., Lopez-Nicolas, A., 2015. Integrated assessment of the impact of climate and land use changes on groundwater quantity and quality in the Mancha Oriental system (Spain). Hydrol. Earth Syst. Sci. 19 (4), 1677–1693.

Qian, H., Li, P., Howard, K.W.F., Yang, C., Zhang, X., 2012. Assessment of groundwater vulnerability in the Yinchuan Plain, Northwest China using OREADIC. Environ. Monit. Assess. 184 (6), 3613–3628.

Qian, H., Wu, J., Zhou, Y., Li, P., 2014. Stable oxygen and hydrogen isotopes as indicators of lake water recharge and evaporation in the lakes of the Yinchuan Plain. Hydrol. Process. 28 (10), 3554–3562.

Ramos, N.F., Folch, A., Fernàndez-Garcia, D., et al., 2020. Evidence of groundwater vulnerability to climate variability and economic growth in coastal Kenya. J. Hydrol. 586, 124920 https://doi.org/10.1016/j.jhydrol.2020.124920.

Rodionov, S., Overland, J.E., 2005. Application of a sequential regime shift detection method to the Bering Sea ecosystem. ICES J. Mar. Sci. 62 (3), 328–332. https://doi.org/10.1016/j.icesjms.2005.01.013.

Sekhar, M., Shindekar, M., Tomer, S.K., et al., 2013. Modeling the vulnerability of an urban groundwater system due to the combined impacts of climate change and management scenarios. Earth Interact. 17 (10), 1–25. https://doi.org/10.1175/2012ei000499.1.

Shamir, E., Megdal, S.B., Carrillo, C., Castro, C.L., Chang, H.-I., Chief, K., Corkhill, F.E., Eden, S., Georgakakos, K.P., Nelson, K.M., Prietto, J., 2015. Climate change and water resources management in the Upper Santa Cruz River, Arizona. J. Hydrol. 521, 18–33.

Taylor, R.G., Scanlon, B., Döll, P., Rodell, M., van Beek, R., Wada, Y., Longuevergne, L., Leblanc, M., Famiglietti, J.S., Edmunds, M., Konikow, L., Green, T.R., Chen, J., Taniguchi, M., Bierkens, M.F.P., MacDonald, A., Fan, Y., Maxwell, R.M., Yechieli, Y., Gurdak, J.J., Allen, D.M., Shamsudduha, M., Hiscock, K., Yeh, P.-F., Holman, I., Treidel, H., 2013. Ground water and climate change. Nat. Clim. Chang. 3 (4), 322–329.

Vallet-Coulomb, C., Séraphin, P., Gonçalvès, J., Radakovitch, O., Cognard-Plancq, A.-L., Crespy, A., Babic, M., Charron, F., 2017. Irrigation return flows in a mediterranean aquifer inferred from combined chloride and stable isotopes mass balances. Appl. Geochem. 86, 92–104.

Vrzel, J., Ludwig, R., Gampe, D., Ogrinc, N., 2019. Hydrological system behaviour of an alluvial aquifer under climate change. Sci. Total Environ. 649, 1179–1188.

Wang, W., Zhang, Z., Duan, L., et al., 2018. Response of the groundwater system in the Guanzhong Basin (central China) to climate change and human activities. Hydrogeol. J. 26 (5), 1429–1441. https://doi.org/10.1007/s10040-018-1757-7.

Wang, W., Zhang, Z., Yin, L., et al., 2021a. Topical Collection: Groundwater recharge and discharge in arid and semi-arid areas of China. Hydrogeol. J. 29 (2), 521–524. https://doi.org/10.1007/s10040-021-02308-0.

Wang, Z., Yang, Y., Chen, G., Wu, J., Wu, J., 2021b. Variation of lake-river-aquifer interactions induced by human activity and climatic condition in Poyang Lake Basin, China. J. Hydrol. 595, 126058. https://doi.org/10.1016/j.jhydrol.2021.126058.

Xu, X., Liu, J., Zhang, S., 2018. China's Multi-Period Land Use Land Cover Remote Sensing Monitoring Dataset (CNLUCC). Data Center for Resources and Environmental Sciences, Chinese Academy of Sciences (http://www.resdc.cn). https:doi.org/10.12078/2018070201.

Xu, Y., Shao, J., Cui, Y., et al., 2015. Application of groundwater modeling systems to the evaluation of groundwater resources in the Yinchuan Plain. Hydrogeol. Eng. Geol. 42 (3), 7–12. https://doi.org/10.16030/j.cnki.issn.1000-3665.2015.03.02.

Xu, W., Su, X., 2019. Challenges and impacts of climate change and human activities on groundwater-dependent ecosystems in arid areas - A case study of the Nalenggele alluvial fan in NW China. J. Hydrol. 573, 376–385. https://doi.org/10.1016/j.jhydrol.2019.03.082.

Yang, Y., Yang, W., Wang, D., 2018. Quaternary distribution characteristics of Yinchuan Basin based on electrical characteristics (in Chinese). Ningxia Eng. Technol. 17 (1), 15–19.

Zhang, X., 2007. Study on water saving potential and water consumption in Yellow River irrigation districts in Ningxia and inner Mongolia autonomous regions (in Chinese). Xi'an University of Technology. Master Thesis,.

Zhang, C., Zhang, B., Li, W., Liu, M., 2014. Response of streamflow to climate change and human activity in Xitiaoxi river basin in China. Hydrol. Process. 28 (1), 43–50.

Zhao, X., Yu, Q., Fei, L., et al., 2015. Laws for water diversion and drainage water volume in Qingtongxia irrigation area (in Chinese). Water Saving Irrigation 3, 73–75.

Zhou, P., Wang, G., Duan, R., 2020. Impacts of long-term climate change on the groundwater flow dynamics in a regional groundwater system: Case modeling study in Alashan, China. J. Hydrol. 590, 125557. https://doi.org/10.1016/j.jhydrol.2020.125557.